LOCKHEED MARTIN ENERGY RESEARCH LIBRARIES

3 4456 0515232 1

ORNL-5488

Experimental Data for Ammonia Condensation on Vertical and Inclined Fluted Tubes

S. K. Combs

OAK RIDGE NATIONAL LABORATORY
CENTRAL RESEARCH LIBRARY
CIRCULATION SECTION
4500N ROOM 175
LIBRARY LOAN COPY
DO NOT TRANSFER TO ANOTHER PERSON
If you wish someone else to see this report, send in name with report and the library will arrange a loan.
UCN-7969 (3 9-77)

OAK RIDGE NATIONAL LABORATORY
OPERATED BY UNION CARBIDE CORPORATION · FOR THE DEPARTMENT OF ENERGY

Printed in the United States of America. Available from
National Technical Information Service
U.S. Department of Commerce
5285 Port Royal Road, Springfield, Virginia 22161
Price: Printed Copy $5.25; Microfiche $3.00

This report was prepared as an account of work sponsored by an agency of the United States Government. Neither the United States Government nor any agency thereof, nor any of their employees, contractors, subcontractors, or their employees, makes any warranty, express or implied, nor assumes any legal liability or responsibility for any third party's use or the results of such use of any information, apparatus, product or process disclosed in this report, nor represents that its use by such third party would not infringe privately owned rights.

ORNL-5488
Dist. Category UC-93

Contract No. W-7405-eng-26

Energy Division
and
Engineering Technology Division

EXPERIMENTAL DATA FOR AMMONIA CONDENSATION ON VERTICAL AND INCLINED FLUTED TUBES

S. K. Combs
Engineering Technology Division

Date Published: January 1979

OAK RIDGE NATIONAL LABORATORY
Oak Ridge, Tennessee 37830
operated by
UNION CARBIDE CORPORATION
for the
DEPARTMENT OF ENERGY

LOCKHEED MARTIN ENERGY RESEARCH LIBRARIES

3 4456 0515232 1

CONTENTS

Page

LIST OF FIGURES v
LIST OF TABLES vi
LIST OF SYMBOLS vii
ABSTRACT ix
ACKNOWLEDGMENTS xi
I. INTRODUCTION 1
II. DESCRIPTION OF EQUIPMENT 3
General Flow Description 3
Test Tubes 5
III. PROCEDURES AND INSTRUMENTATION 12
Steady-State Operation 12
Instrumentation 13
IV. ANALYSIS 15
Overall Condensing Coefficients 15
Individual Condensing-Side Coefficients 16
V. RESULTS AND DISCUSSION 19
Tube Length Effects 19
Inclined Condenser Tubes 20
Doubly Fluted Tubes 25
SUMMARY 29
REFERENCES 30
APPENDIX A — SAMPLES OF DATA REDUCTION 31
Physical Properties for Ammonia 31
Fluted Tube 31
APPENDIX B — WILSON-PLOT RESULTS 39
APPENDIX C — EXPERIMENTAL DATA 43
APPENDIX D — SI CONVERSION FACTORS 53

LIST OF FIGURES

FIGURE		Page
1-1.	Fluted tube principle of operation (condensation mode) — surface tension forces acting to push condensate from crests into troughs	2
2-1.	Schematic diagram of experimental apparatus	4
2-2.	Test facility	6
2-3.	Details of the test section	7
2-4.	Photographs of tube samples — tubes A and H	9
2-5.	Photographs of tube samples — tube F with and without a skirt	10
5-1.	Comparison of heat transfer performance between tube F (48 corrugations) and duplicate tubes containing equally spaced drainage skirts — h* vs Q/A	21
5-2.	Comparison of heat transfer performance between tube F (48 corrugations) and duplicate tubes containing equally spaced drainage skirts — Q vs ΔT*	22
5-3.	Comparison of heat transfer performance of a smooth and a fluted tube for vertical and 30° off vertical orientations — h* vs Q/A	23
5-4.	Comparison of heat transfer performance of a smooth and a fluted tube for vertical and 30° off vertical orientations — Q vs ΔT*	24
5-5.	Heat transfer performance of tube H [1.2 m (4-ft) long, 42 outside and 34 inside flutes) — ammonia condensing on the outside surface and water flowing through an annulus inside the tube	26
5-6.	Heat transfer performance of tube H [1.2 m (4-ft) long, 42 outside and 34 inside flutes] — ammonia condensing on the outside surface and water flowing through the inside of the tube (no rod inside the tube)	27
A-1.	Wilson plot for ammonia condensing on tube E (60 square ridges) — Runs 717-051E to 717-056E	37

LIST OF TABLES

TABLE		Page
2-1.	Characteristics of tubes	8
A-1.	Sample of experimental data — ammonia condensing on tube E	32
A-2.	Sample information for the Wilson plot — ammonia condensing on tube E	35
B-1.	Summary of experimental conditions and results from Wilson plots for ammonia condensing on tube F-7 (a duplicate of tube F with 7 skirts)	40
B-2.	Summary of experimental conditions and results from Wilson plots for ammonia condensing on tube AT (smooth tube 30° off vertical)	41
B-3.	Summary of experimental conditions and results from Wilson plots for ammonia condensing on tube FT (F 30° off vertical)	42
C-1.	Experimental data for ammonia condensing on tube F-7 (a duplicate of tube F with 7 skirts)	44
C-2.	Experimental data for ammonia condensing on tube AT (tube A — 30° off vertical)	46
C-3.	Experimental data for ammonia condensing on tube FT (tube F — 30° off vertical)	48
C-4.	Experimental data for ammonia condensing on tube H (0.5-in.-OD rod on water side)	49
C-5.	Experimental data for ammonia condensing on tube HN (tube H with no rod on water side)	51

LIST OF SYMBOLS

a_o	y-intercept on the Wilson plot representing the composite resistance of the condensing side and wall, Eq. (4-11)
a_1	slope of the line on the Wilson plot
A	heat transfer surface area of test tube
A_c	cross-sectional flow area of the annulus in the test section
c_p	specific heat
D	tube diameter
D_r	diameter of rod inserted through center of test section
F	volume flow rate
h	average or mean individual heat transfer coefficient
h_{fg}	latent heat of vaporization
h^*	composite condensing heat transfer coefficient including both vapor side and wall
k	thermal conductivity
$\dot{m}$	mass flow rate
P	pressure
P_t	outside perimeter of tube
Q	heat load
Q/A	heat flux
r	radius
R	resistance to heat flow
T	temperature
ΔT	temperature difference
$\overline{\Delta T}$	mean temperature difference between the condensing vapor and coolant
ΔT^*	composite condensing temperature difference including both vapor side and wall

U	overall condensing heat transfer coefficient
v	water velocity

Subscripts

avg	average
c	ammonia condensate
fi	inside fouling
fo	outside fouling
i	inside
in	inlet
o	outside
out	outlet
sat	saturation
v	vapor; vapor (condensing) side
w	water; water side
wall	wall; surface

ABSTRACT

Heat transfer experiments were run to evaluate the performance of single fluted tubes with ammonia condensing on the outside. Data are presented for tubes of 2.54-cm (1-in.) nominal diameter and 1.2 m (4 ft) in length including (1) tests with a vertical fluted tube with seven equally spaced drainage skirts — "effective" condensing length of 0.15 m (0.5 ft), (2) tests with both a smooth and a fluted tube inclined 30° off vertical, and (3) tests with a doubly fluted tube. The results for the tube with drainage skirts showed that for ammonia there was no advantage in going to shorter condensing lengths [<1.2 m (4 ft)] in the range of heat fluxes tested [5000–50,000 W/m^2 (1600–16,000 $Btu/hr \cdot ft^2$)]. For the inclined tests, the film condensation coefficients for the smooth tube were more than doubled over results for a vertical smooth tube; whereas, for the inclined fluted tube, the heat transfer performance was slightly lower than for a vertical orientation. Overall heat transfer coefficients are presented for the doubly fluted tube over a range of water velocities and heat loads; data are given for two inside tube (water-side) configurations — one for full flow through the tube and one for flow through an annulus.

ACKNOWLEDGMENTS

This investigation was performed at the Oak Ridge National Laboratory operated by the Union Carbide Corporation for the Department of Energy. This study was a part of the general program on Low-Temperature Heat Utilization being performed by ORNL for the DOE Division of Central Solar Technology, Ocean Systems Branch. The author is particularly grateful for the contributions of the following persons: J. W. Michel (Program Manager), R. W. Murphy (Project Engineer), and R. N. Lyon (ORNL Consultant) for their helpful suggestions; R. L. Linkous and C. V. Hardin (Project Technicians) for operation of the test equipment and collection of data; and Dolores Eden for her assistance in organizing the materials for the report and for typing the manuscript.

CHAPTER I

INTRODUCTION

A previous report[1] presented heat transfer data for ammonia condensing on both smooth and fluted vertical tubes of 4-ft length. The data showed that fluted tubes could significantly increase condensing coefficients (up to 7.2 times) over conventional smooth tubes for a given heat flux. Data were also reported for a fluted tube with a skirt attached at the midpoint of the condensing length, dividing the 4-ft length into "effective" lengths of 2 ft. This report presents additional condensation experiments with ammonia including further data on the effect of tube length, data for an inclined tube orientation (30° off vertical) for both a smooth and a fluted tube, and data for a doubly fluted tube.

Background material for this study was given in the previous report[1] along with detailed descriptions of the equipment, procedures, and instrumentation, all of which remained the same throughout this study. Therefore, only brief descriptions are provided within. In a similar study, Combs, Mailen, and Murphy[2] presented extensive experimental data for various refrigerants condensing on vertical fluted tubes.

The emphasis on fluted tubes stemmed from the performance efficacy identified in water studies, such as that of Alexander and Hoffman.[3] The principle of operation (condensation mode) for the fluted tubes is pictorially shown in Fig. 1-1. The condensate film is subject to surface tension forces acting to push it from the crests into the troughs. This results in the major portion of the crest having a very thin film of condensate which greatly reduces the resistance to heat flow through the crest area. The condensate in the troughs is channeled off by gravity with the heat flow through this area somewhat less. The net effect is an improvement in heat transfer performance of fluted tubes over conventional smooth tubes.

ORNL-DWG 77-5469A

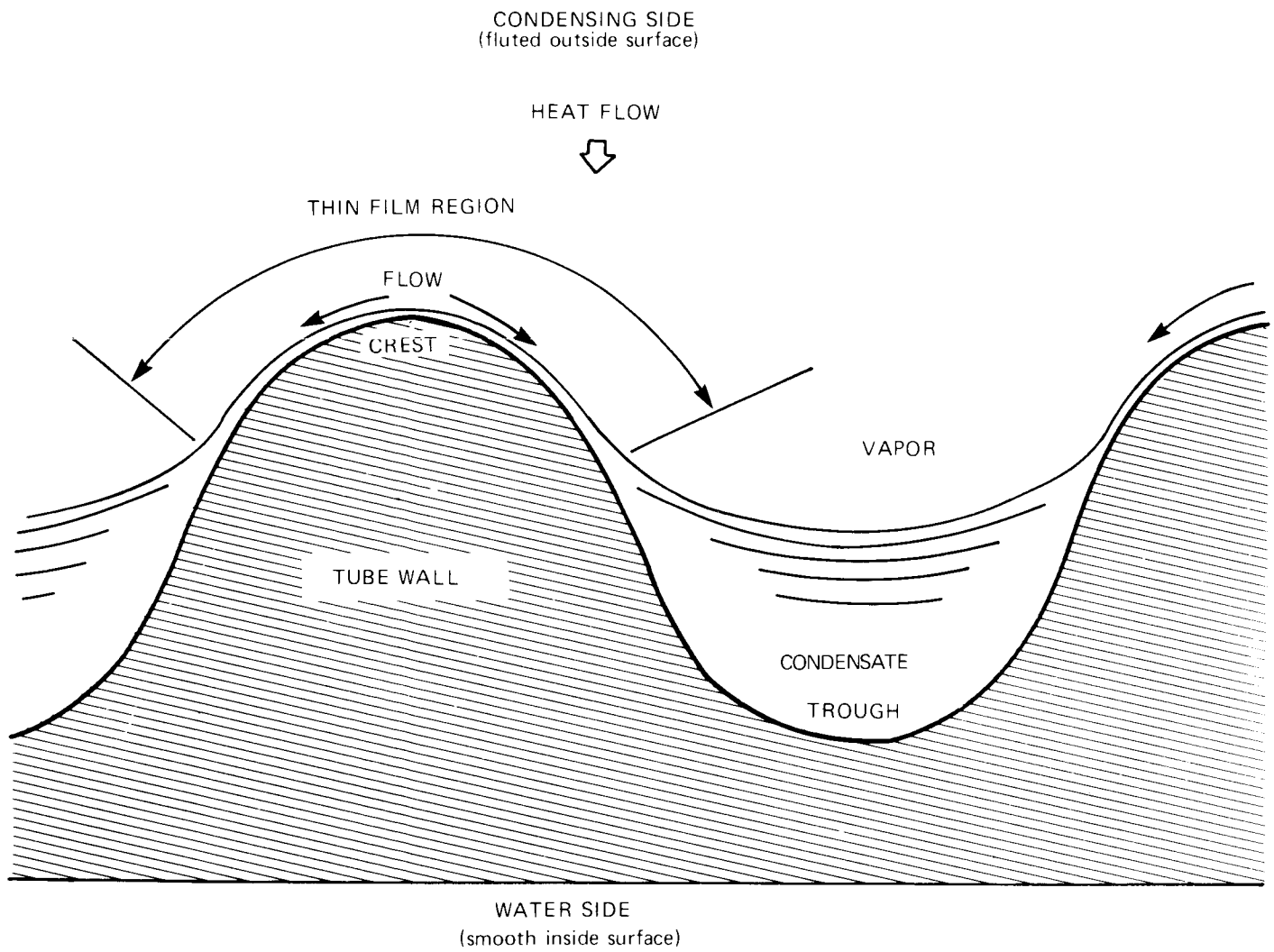

Fig. 1-1. Fluted tube principle of operation (condensation mode) — surface tension forces acting to push condensate from crests into troughs.

CHAPTER II

DESCRIPTION OF EQUIPMENT

Equipment used in this investigation is shown schematically in Fig. 2-1. The system was designed for a heat load of 5 kW and consisted of three circuits — an ammonia loop, a primary cooling loop, and a secondary cooling loop. The ammonia loop was designed for a maximum operating pressure and temperature of 250 psia and 110°F. The test section, a single-tube vertical condenser, was built to accommodate tubes of 1- or 2-in.-nominal diameter and 4 ft in length. The system was manually controlled, and the heat load was set by the power input to the boiler. The ammonia loop was constructed of stainless steel to minimize compatibility problems. View ports on the test section permitted visual observation of the condensing surface with the aid of a light at suitable locations. Water served as the coolant in both the primary and secondary cooling loops. The primary coolant removed the heat from the tube in the test section; and in turn, the heat was transferred to the secondary coolant.

General Flow Description

Flow directions in the system are indicated by arrows in Fig 2-1. Typically, the ammonia was vaporized in the boiler and passed through an entrainment separator before entering the condensing test section. The vapor entered the top of the test section, and the liquid (collected in the separator) returned to the boiler. The vapor condensed on the outer surface of the test tube in the test section and formed a falling film of liquid. The liquid condensate exited at the bottom of the test section, passed through a condensate measuring station, and returned to the bottom of the boiler to complete the closed loop. A pump was not needed for the circulation of the ammonia since the liquid head in the test-section side of the loop furnished the driving force required for flow through the condensate measuring station.

In the primary cooling loop, a centrifugal pump transferred demineralized water from a storage tank to the bottom of the test section and

ORNL–DWG 77–12422

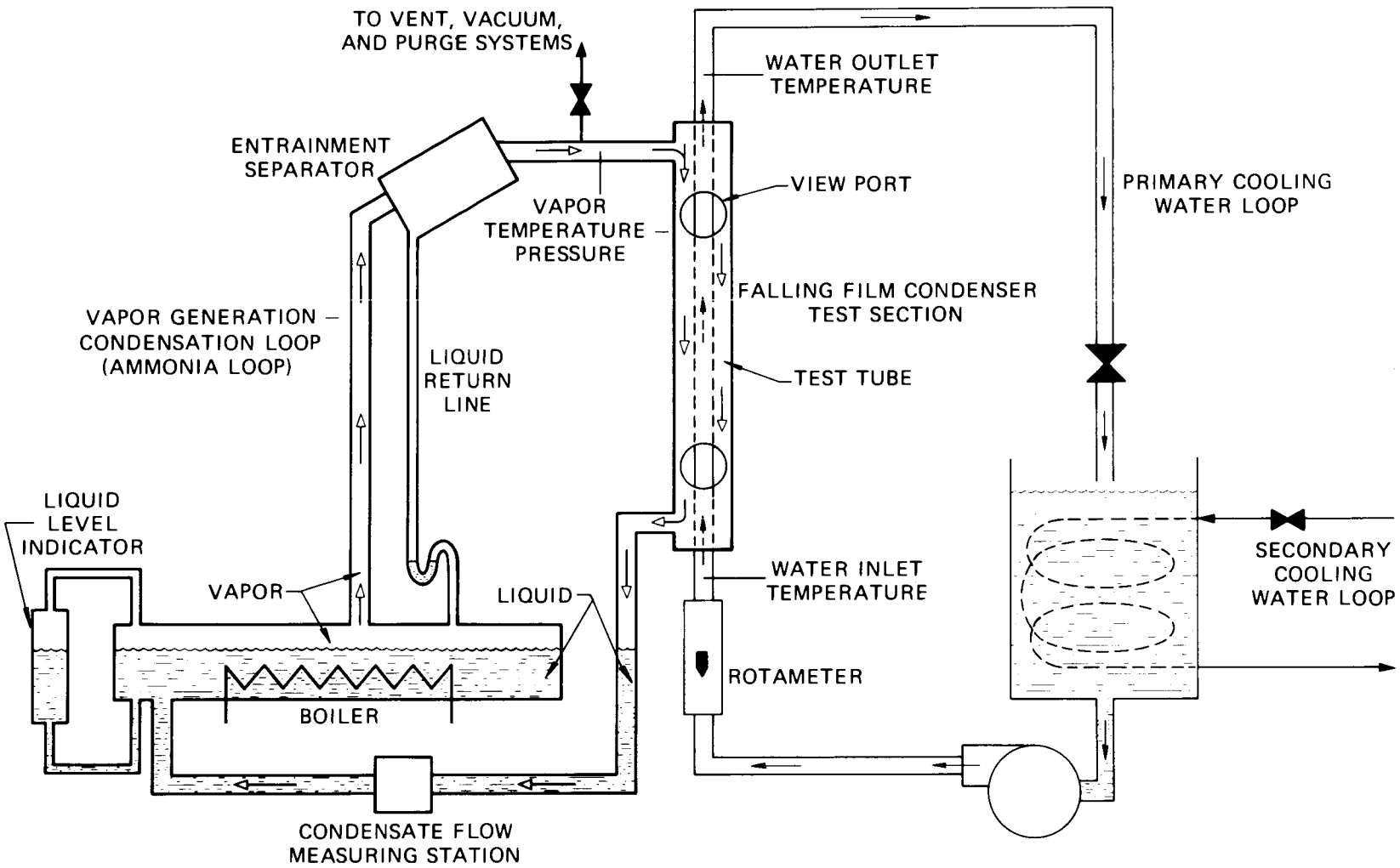

Fig. 2-1. Schematic diagram of experimental apparatus.

upward through the test tube. The primary cooling flow was measured by rotameters upstream of the test section and controlled by a hand valve located downstream of the test section. From the top of the test section, the water returned to the storage tank to complete the closed loop.

The secondary cooling loop removed the heat load from the system by transferring the heat from the primary cooling water to plant process water. Primary cooling water recirculating through the storage tank dumped heat to secondary cooling water which passed through a cooling coil in the tank and then discharged to a drain. The flow rate of the secondary coolant was regulated by a hand valve located downstream of the cooling coil.

Figure 2-2 pictures the system in an overall view, and Fig. 2-3 gives more detail of the test section. These photographs do not show the insulation that was installed prior to experimental operation to minimize heat losses.

Test Tubes

The performance of four aluminum tubes (1-in.-nominal diameter) was previously reported.[1] Letter designations (A, E, F, and G) were used to identify the tubes. Additional data for three tubes (A, F, and H) are reported in this study. Detailed descriptions of the tubes are given in Table 2-1, and enlarged photographs of tube samples are presented in Figs. 2-4 and 2-5. Tube H was an aluminum tube with 42 outside and 34 inside rounded flutes (corrugations); therefore, tube H was the only tube tested that contained inside flutes. For tubes F and H, the outside perimeters were estimated as the length of thin tape required to fit tightly around the outside surface of the tube. The active length of smooth tube A was 48 in., while for the fluted tubes the effective length was 46 in. About 1 in. at each end of the fluted test tubes was taken up by sleeve and installation clearances.

A duplicate of tube F (designated as tube F-7) was also tested with seven equally spaced neoprene skirts attached to the outside surface. These tests were conducted to obtain some further indication of the effect of tube length on the condensing heat transfer performance of fluted tubes.

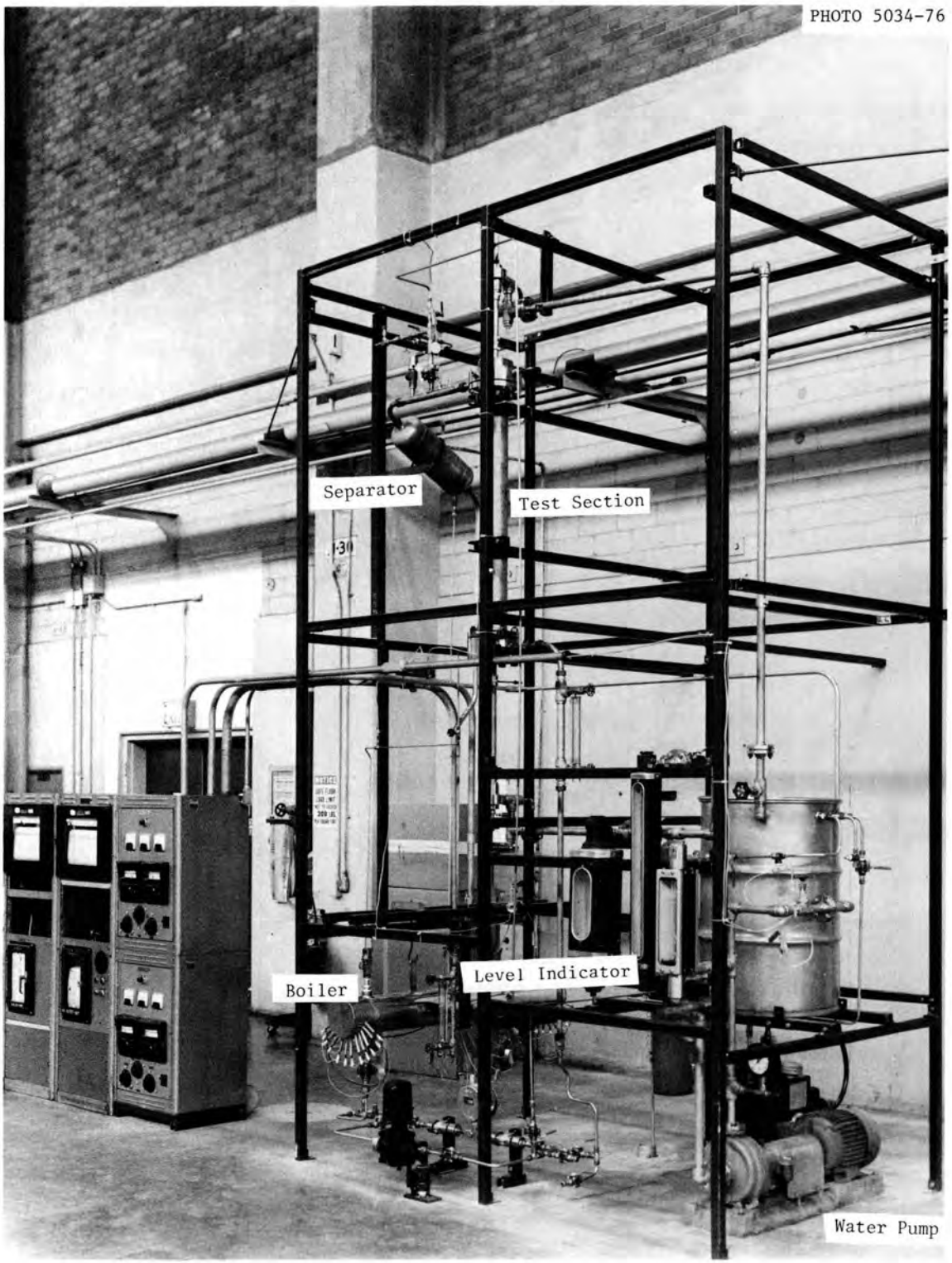

Fig. 2-2. Test facility.

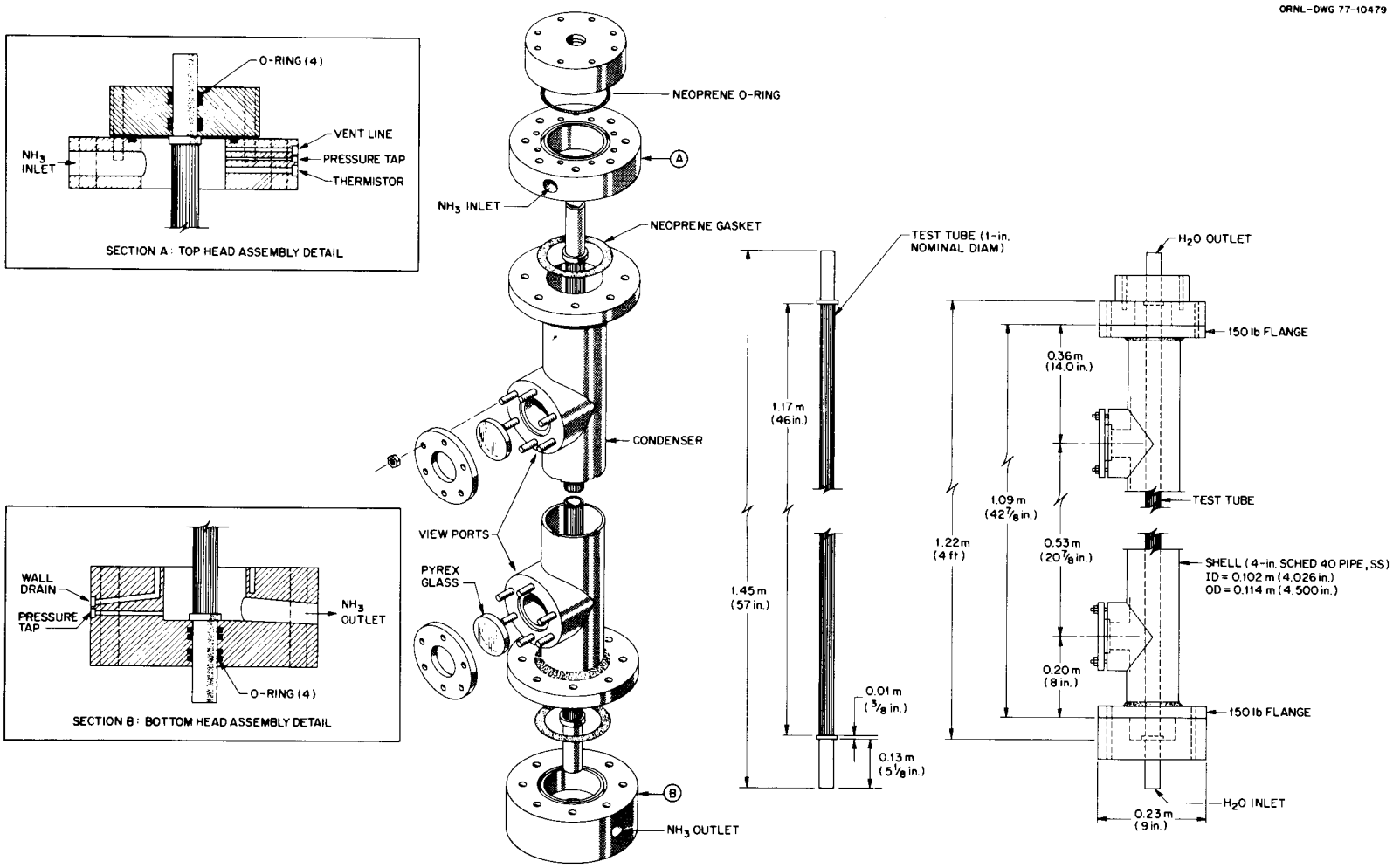

Fig. 2-3. Details of the test section.

Table 2-1. Characteristics of tubes.

Cross section	Tube designation	Inside diameter		Outside perimeter		Outside surface area		Number of outside flutes
		cm	(in.)	cm	(in.)	m^2	(ft^2)	
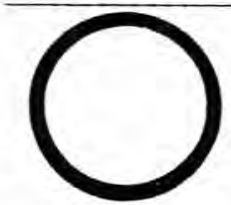	A	2.21	(0.87)	7.98	(3.14)	0.0974	(1.05)	—
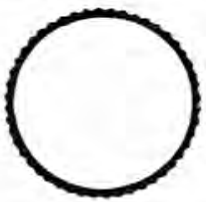	F	2.29	(0.90)	8.26	(3.25)	0.0964	(1.04)	48
	H	—	—	14.00	(5.51)	0.163	(1.76)	42[a]

[a]Also contains 34 inside flutes.

ORNL PHOTO 7436–78

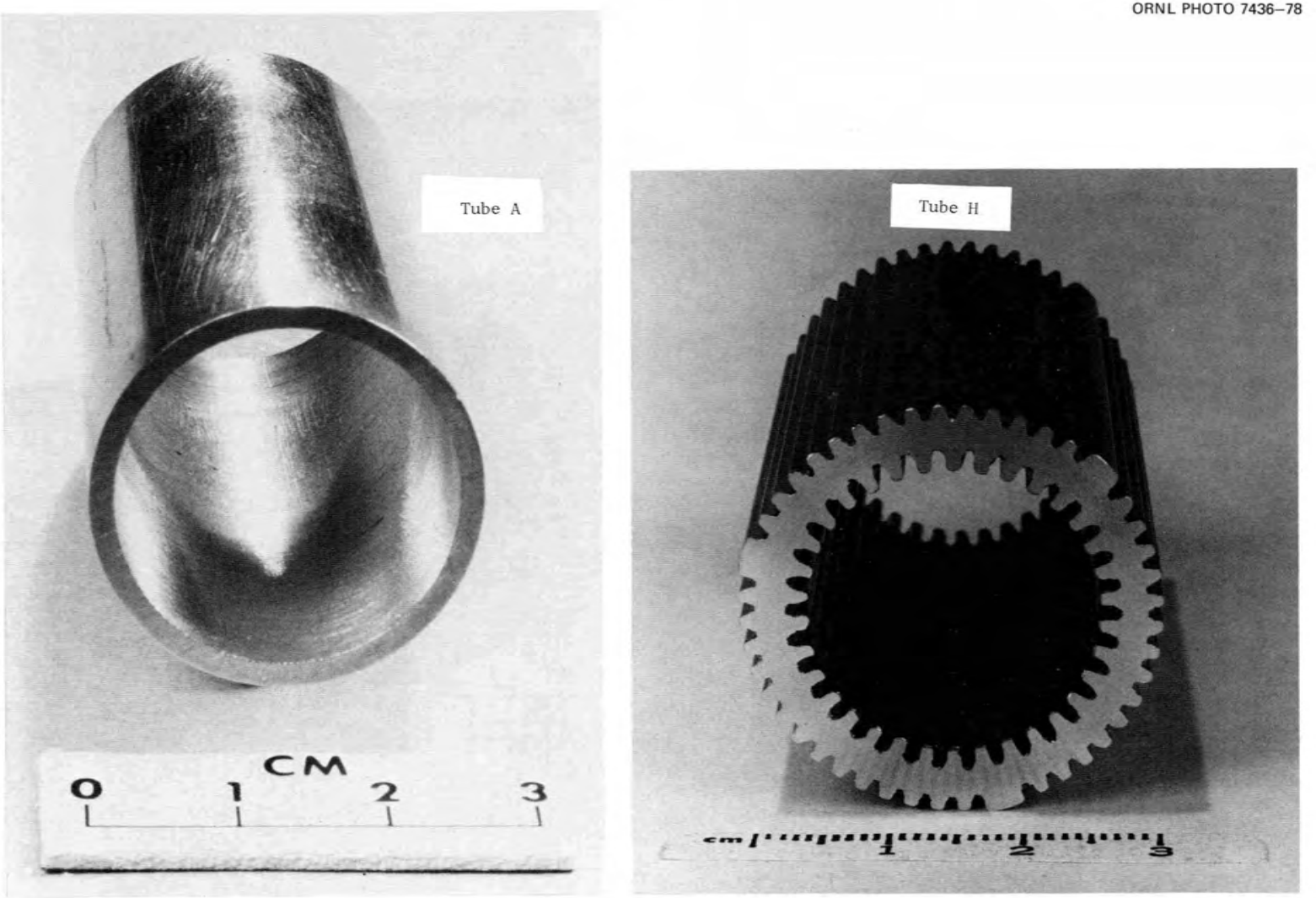

Fig. 2-4. Photographs of tube samples — tubes A and H.

ORNL PHOTO 7437–78

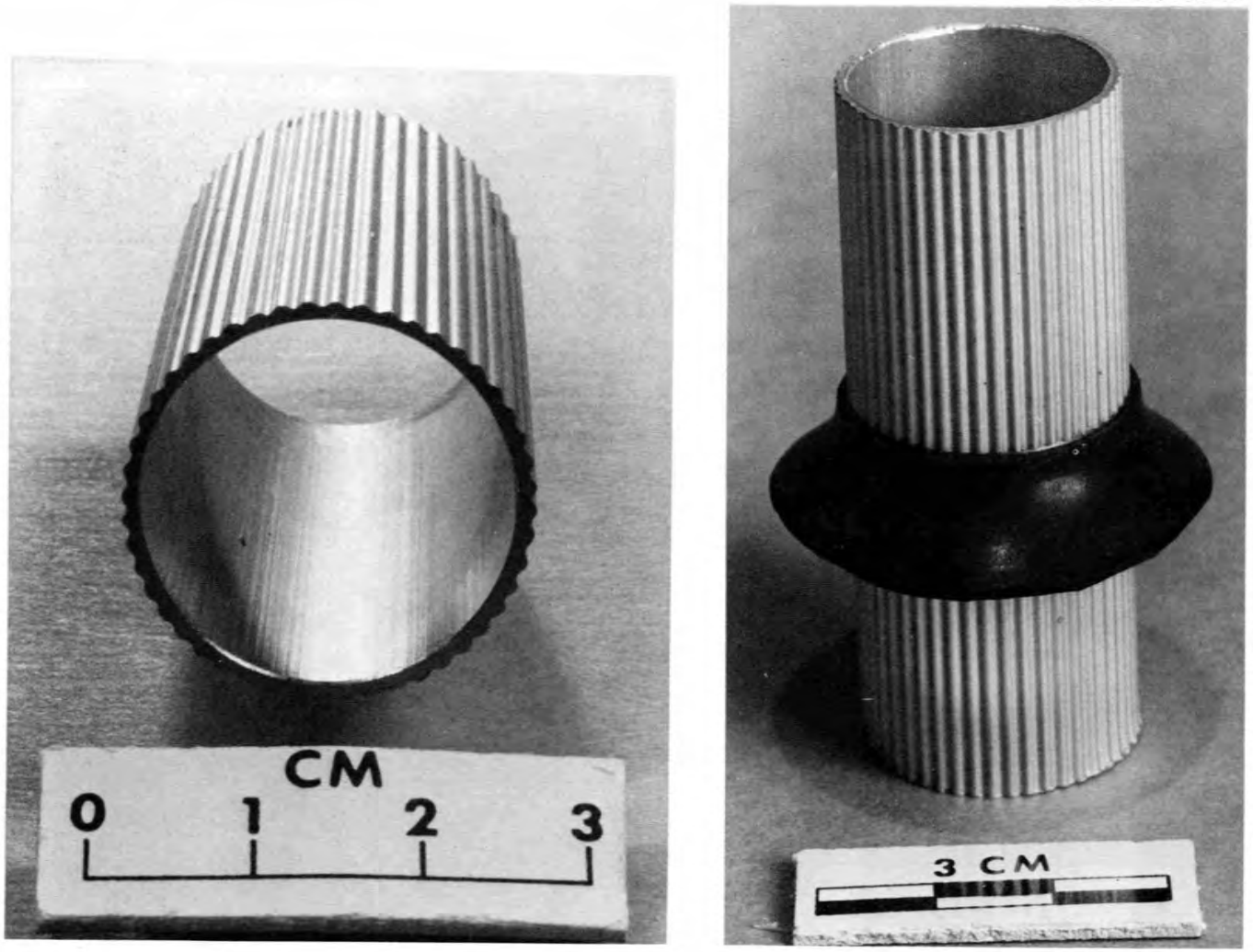

Fig. 2-5. Photographs of tube samples — tube F with and without a skirt.

In the previous report, data were reported for tube F-1 (F with 1 skirt). An enlarged photograph of a tube sample is presented in Fig. 2-5 to show the skirt configuration.

In most tests, a stainless steel rod of 0.50-in. outside diameter was installed through the center of the test section (inside the test tube) in order to decrease the hydraulic diameter and increase the velocity for a given primary cooling volume flow. Both of these variations tended to increase the heat transfer coefficients on the water side; and, as a result, improve the accuracy of the Wilson-plot technique[4] used to interpret the experimental data. For example, with a smooth 0.87-in.-ID tube (designated tube A), insertion of the 0.50-in.-OD rod decreased the hydraulic diameter by 57% and increased the velocity by 49%.

CHAPTER III

PROCEDURES AND INSTRUMENTATION

Heat transfer rates and temperature differences in the condenser were calculated from experimental data taken during steady-state operations (see Appendix A for sample calculations). Accurate temperature measurements were critical, since it was sometimes necessary to measure very small temperature differences ($\sim$0.2°F) to within ±0.04°F to obtain reliable heat balances. Further, small condensate flows (as low as 0.01 gpm) had to be measured accurately for good interpretation of the experimental data.

Steady-State Operation

The heat rate to the boiler was controlled by Variacs which regulated the voltage across the boiler. After setting the heat rate to the boiler, the primary cooling flow rate was adjusted by the valve downstream of the test section. Since the inlet temperature of the secondary cooling water was fixed by the plant process water conditions, the flow rate of the secondary cooling water was used to control the temperature of the primary cooling water. This, in turn, controlled the vapor temperature in the test section. Temperatures and pressures throughout the system were monitored to determine when steady-state conditions existed; steady state was assumed when there was no significant change in temperatures (±0.1 to 0.2°F) throughout the system over a five- to ten-minute span.

Once a steady state was achieved, the experimental data were recorded. The information recorded included the vapor temperature and pressure in both the condenser and boiler, the flow rate and temperature of the condensate, the inlet and outlet temperatures and flow rates of the primary and secondary coolants, and the voltage and current to boiler. These experimental data were then used to calculate heat transfer rates and temperature differences in the system and to check pressure-temperature values against saturation data in the literature (see Appendix A for examples).

After all of the data were recorded for a given steady-state situation, the flow rate of the primary cooling water was changed and the flow rate of the secondary cooling water adjusted (range of 0 to 4 gpm) until the system reached a new steady state. When this steady state was reached, the experimental data were again recorded. The same procedure was followed until data were collected for at least three coolant flow rates at the same boiler heat rate. In the experiments, the primary cooling flow rates ranged from 3.0 to 34.0 gpm. The heat rate to the boiler was then changed, and the entire procedure was repeated at the new heat rate.

Instrumentation

The voltage across the boiler was measured by voltmeters, and the current was measured by ammeters. The voltage and current information was used to control and monitor the power input to the boiler. Pressures in the boiler and the condenser were measured with gauges (main instrument was a U. S. Gauge, Dial No. 33006) capable of spanning the range of 0 to 300 psig. The ammonia loop was also equipped with a compound gauge for reading low pressures and subatmospheric pressures.

For temperature measurements, the system was equipped with chromel-alumel thermocouples; thermocouples were located in the liquid and vapor of the boiler, in the vapor feed to the test section, in the inlet and outlet of both cooling water loops, near the condensate measuring station, and on each heater. The recorded thermocouple data were used in deciding when the system reached a steady state. In addition, both a quartz thermometer and a thermistor were located in the vapor feed to the test section and in the inlet and outlet of the primary cooling water. Also, a quartz thermometer was located near the condensate measuring station. The information from the quartz thermometers (Hewlett Packard, Model 2801A) and the thermistors (Thermometrics, Part No. S-10-4-wire) was used for data reduction because of the greater accuracy attributed to these instruments. However, the experimental data from the three sets of temperature measuring instruments were checked against each other to increase the confidence in the temperature measurements.

The condensate flow in the ammonia loop was measured by two instruments: an integral orifice meter and a turbine flow transducer. These two instruments were located in parallel with piping permitting the routing of the flow through either device. An integral flow orifice assembly was used to adapt a pneumatic d/p cell transmitter (Foxboro Model 15A) for measurement of low flow rates. With the integral orifice meter, it was necessary to change orifice plates for various flow ranges. A turbine flow transducer (Flow Technology, Model FTM-NX3-LJS) equipped with a range extending amplifier (Flow Technology, Model LFA-300AX) facilitated operation. The range extending amplifier made it possible to cover the full range of interest (0.01 to 0.2 gpm) with only one instrument. Measurements from the turbine flow transducer were used in reducing the data with the integral orifice meter results used as a check. The two values always agreed to within a few percent.

The primary cooling water flow was measured by rotameters upstream of the test section. The information from these two rotameters was utilized in the data reduction (see Appendix A, Table A-1). The secondary cooling water was measured by a small rotameter upstream of the cooling coil.

CHAPTER IV

ANALYSIS

Overall Condensing Coefficients

The heat transfer rate in the condenser can be written:

$$Q = UA\overline{\Delta T} \quad , \tag{4-1}$$

where U is the overall heat transfer coefficient, $\overline{\Delta T}$ is the mean temperature difference between the condensing vapor and the primary cooling water, and A is surface area of the test tube. The heat transfer rate can be computed from either the condensate mass flow rate ($\dot{m}_c$) or from the product of mass flow rate ($\dot{m}_w$) and temperature rise (ΔT_w) of the primary cooling water; thus,

$$Q = \dot{m}_c \, h_{fg} \tag{4-2}$$

and

$$Q = \dot{m}_w \, c_{pw} \, \Delta T_w \quad , \tag{4-3}$$

where h_{fg} is the latent heat of ammonia, and c_{pw} is the heat capacity of water. In this analysis, all physical property data for ammonia were taken from ASHRAE handbooks,[5-7] where ammonia is designated as Refrigerant 717.

The arithmetic mean difference is used for $\overline{\Delta T}$, since in most cases the temperature difference across the water was relatively small. Therefore, assuming saturated vapor:

$$\overline{\Delta T} = T_v - (T_{w,in} + T_{w,out})/2 \quad , \tag{4-4}$$

where T_v is the ammonia vapor temperature and the second term on the right is the average of the inlet water temperature ($T_{w,in}$) and the outlet water temperature ($T_{w,out}$).

The overall coefficient can be computed from Eq. (4-1) using either Eq. (4-2) or Eq. (4-3) to calculate Q. Defining an overall coefficient (U_o) based on the outside surface area (A_o) and rearranging Eq. (4-1):

$$U_o = \frac{Q}{A_o \, \overline{\Delta T}} \quad . \tag{4-5}$$

The next step in the analysis is the evaluation of individual condensing-side coefficients from the overall coefficients.

Individual Condensing-Side Coefficients

A technique introduced by Wilson[4] in 1915 was used as the method of analysis in this study; this is a graphical method of interpreting overall coefficients of heat transfer in surface condensers such that individual condensing-side coefficients can be evaluated. The following treatment presents the method and describes the application to the experimental data in this study.

The overall resistance to heat flow ($\Sigma R = 1/U$) in a condenser is equal to the sum of the individual resistances; thus,

$$1/U = R_v + R_{fo} + R_{wall} + R_{fi} + R_w \ , \tag{4-6}$$

where R_v is the resistance on the vapor (condensing) side, R_{wall} that of the wall, R_w that on the water side, and R_{fo} and R_{fi} account for any fouling on the outside and inside surfaces of the tube, respectively. Introducing individual average heat transfer coefficients (h), neglecting any fouling, and correcting for differences in areas, the overall coefficient based on the outside surface area is represented by:

$$\frac{1}{U_o} = \frac{1}{h_v} + R_{wall} + \frac{A_o}{h_w A_i} \ , \tag{4-7}$$

where A_i is the inside surface area of the tube, h_v is the vapor-side heat transfer coefficient based on the outside tube area, and h_w is the water-side heat transfer coefficient based on the inside tube area. For a smooth tube, the wall resistance based on the outside tube area is given by:

$$R_{wall} = r_o \, \ell n(r_o/r_i)/k \ , \tag{4-8}$$

where r_o and r_i are the outside and inside radii of the tube, respectively, and k is the thermal conductivity of the tube wall.

Neglecting the effects of changes in water temperature, the water-side resistance ($1/h_w$) can be taken as a function of the water velocity (v). For turbulent flow of water, this can be expressed as

$$1/h_w \propto 1/v^{0.8} \quad ,$$

and thus, Eq. (4-7) can be rewritten:

$$\frac{1}{U_o} = \frac{1}{h_v} + R_{wall} + a_1 \, v^{-0.8} \; . \tag{4-9}$$

If, following Wilson, the sum of the first two resistances $(1/h_v + R_{wall})$ is taken as approximately constant, Eq. (4-9) becomes:

$$\frac{1}{U_o} = a_o + a_1 \, v^{-0.8} \quad . \tag{4-10}$$

In this form, a plot of $1/U_o$ vs $1/v^{0.8}$ on ordinary rectangular coordinates should give a straight line from which the constants a_o and a_1 can be determined. Thus, the constant a_o is given by the y-intercept on the Wilson plot and corresponds to the sum of the first two resistances (vapor side plus wall) in Eq. (4-9):

$$a_o = \frac{1}{h_v} + R_{wall} \; . \tag{4-11}$$

The constant a_1 is the slope of the straight line on the Wilson plot.

For a smooth tube, Eq. (4-8) can be used to calculate a wall resistance, and h_v can be computed from Eq. (4-11). However, for fluted tubes, it is very difficult to estimate the contribution of the wall due to the more complicated wall geometry and heat distribution. Accordingly, the coefficients for the fluted tubes are reported as a composite condensing coefficient (h*) that includes both the vapor-side resistance and the wall resistance:

$$h^* = \frac{1}{(1/h_v) + R_{wall}} \tag{4-12}$$

or

$$h^* = \frac{1}{a_o} \; . \tag{4-13}$$

The corresponding composite condensing temperature difference is given by:

$$\Delta T^* = \frac{Q}{h^* A_o} , \tag{4-14}$$

and represents the temperature difference between the vapor and the inside wall of the test tube. A more detailed treatment of this section can be found in Ref. 1.

CHAPTER V

RESULTS AND DISCUSSION

Experimental tests in this study were divided into three types: (1) tests on a vertical fluted tube with seven equally spaced drainage skirts, (2) tests on both smooth and fluted tubes that had been tilted 30° off vertical, and (3) tests with a doubly fluted tube. Condensing experiments (274 runs) are documented in Appendix C (Tables C-1 through C-5), where the experimental data are tabulated along with the overall condensing coefficients. Heat balance checks are also listed in Appendix C; over 90% of the runs were better than ±5%; and all of the runs were better than ±10%. Wilson-plot results for the tubes with smooth inside surfaces are presented in Appendix B, and sample Wilson plots are given in Appendix A along with sample calculations.

Parameter ranges for the experiments were as follows:

Condensing temperature	299–316 K (79–110°F)
Condensing pressure	1.1×10^6 to 1.7×10^6 Pa (153–245 psia)
Heat load	760–5300 W (2600–18,000 Btu/hr)
Heat flux	4700–54,000 W/m^2 (1500–17,000 Btu/hr·ft^2)

All parameters were based on total outside condensing surface area. Condensation data are presented in two dimensional forms in this section. One dimensional presentation, heat transfer coefficient vs heat flux, is useful for describing experimental heat transfer ranges. Also, since both the ordinate and abscissa are based on total outside tube surface area, results are helpful in determining whether the observed augmentation is merely an area effect. The second dimensional form, heat load vs condensing temperature difference, is useful for particular design considerations, since "credit" is allowed for the increased surface area of fluted tubes.

Tube Length Effects

In the previous report,[1] data were presented for ammonia condensing on tube F (48 outside corrugations, 4 ft long) and tube F-1 (a duplicate

of tube F with one drainage skirt attached to the midpoint of the condensing length — "effectively" 2 ft long). In Figs. 5-1 and 5-2, the previous data for tubes F and F-1 are plotted along with the present data for tube F-7 (a duplicate of tube F with seven equally spaced drainage skirts). Data for a smooth tube (A) are also shown for comparison. The seven skirts divide the 4-ft length into "effectively" eight equal lengths of 0.5 ft. As indicated in Figs. 5-1 and 5-2, the use of skirts has no significant effect on the heat transfer performance; the data for all three "effective" lengths (4 ft, 2 ft, and 0.5 ft) are very similar, and the data with skirts fall within the normal scatter of the data for tube F without skirts.

Recent work at the Oak Ridge National Laboratory with refrigerants[2] had indicated significant effects of tube length on heat transfer performance with shorter condensing lengths improving the heat transfer performance. The decrease in heat transfer performance for longer condensing lengths was attributed to liquid flooding of the drainage channels or troughs. However, the larger latent heat of vaporization for ammonia compared to the refrigerants ($\sim$5 to 10 times greater) results in less condensate at the same heat flux. The ammonia data suggest that the 4-ft fluted tube is not near the flooding stage, and shorter condensing lengths offer no advantage for the heat flux range tested. The skirts should provide improvement at higher heat fluxes where flooding would be more pronounced.

Inclined Condenser Tubes

Experiments were run to determine the effect of tube orientation on the condensing heat transfer performance. Thus, series of tests were made with tubes A (smooth) and F (48 outside corrugations) in which the condensing test section had been inclined at 30° from the vertical orientation. The results for the inclined tubes are shown in Figs. 5-3 and 5-4 along with the previous data[1] for the vertical orientation. For the smooth tube (A), the heat transfer performance of the inclined tube is significantly greater than that of the vertical tube (approximately doubled over the full heat flux test range). In contrast, the heat

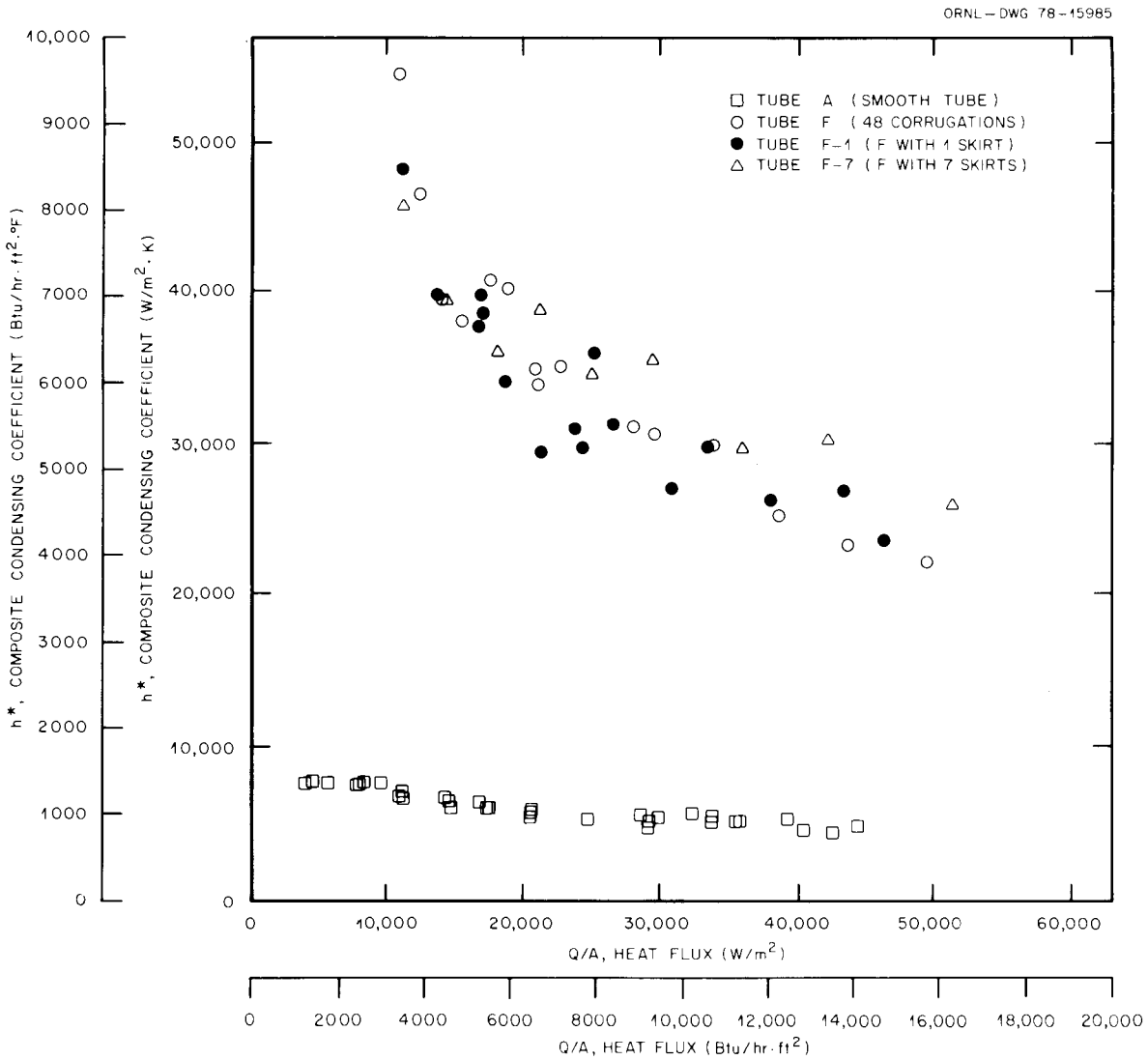

Fig. 5-1. Comparison of heat transfer performance between tube F (48 corrugations) and duplicate tubes containing equally spaced drainage skirts — h* vs Q/A.

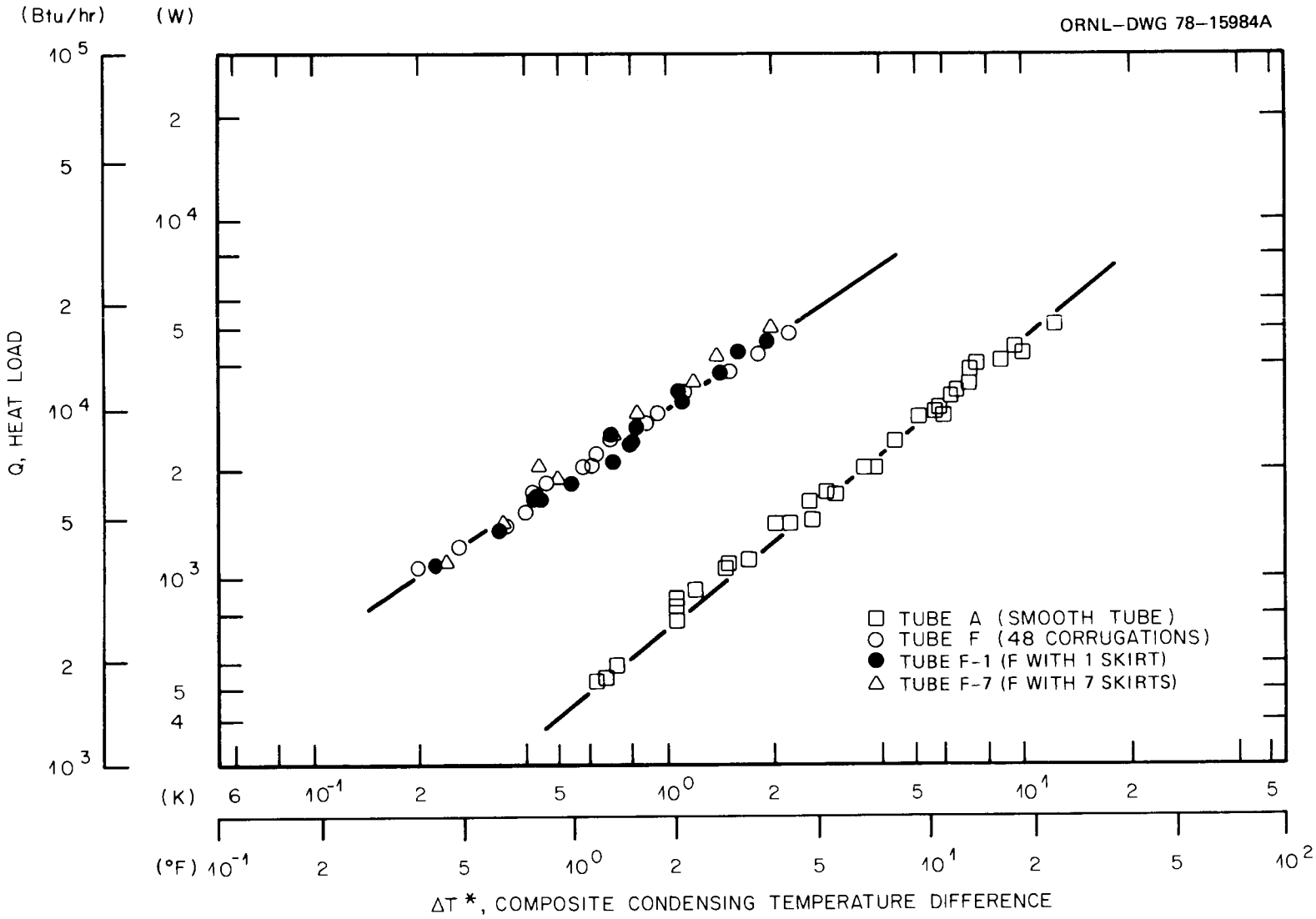

Fig. 5-2. Comparison of heat transfer performance between tube F (48 corrugations) and duplicate tubes containing equally spaced drainage skirts — Q vs ΔT*.

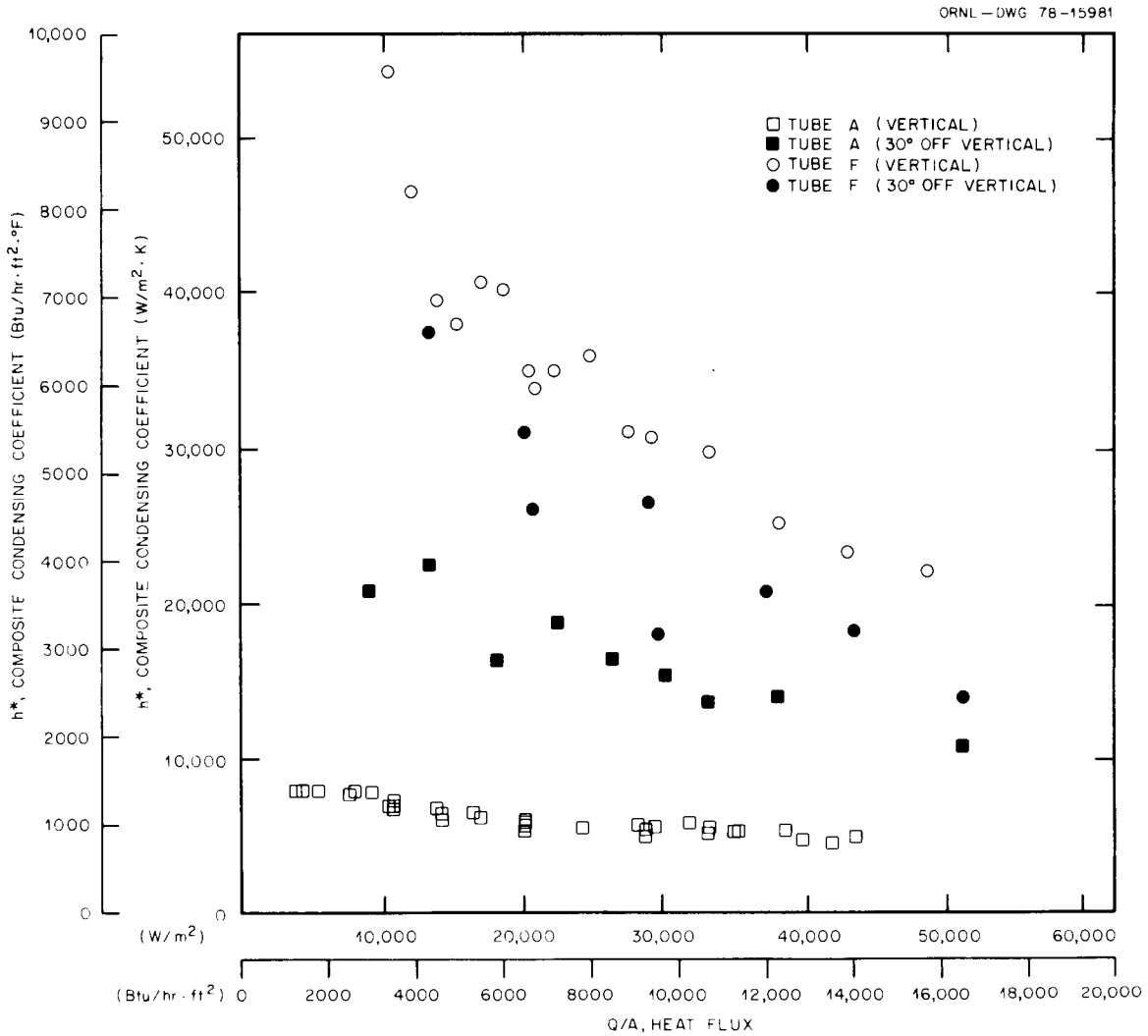

Fig. 5-3. Comparison of heat transfer performance of a smooth and a fluted tube for vertical and 30° off vertical orientations — h* vs Q/A.

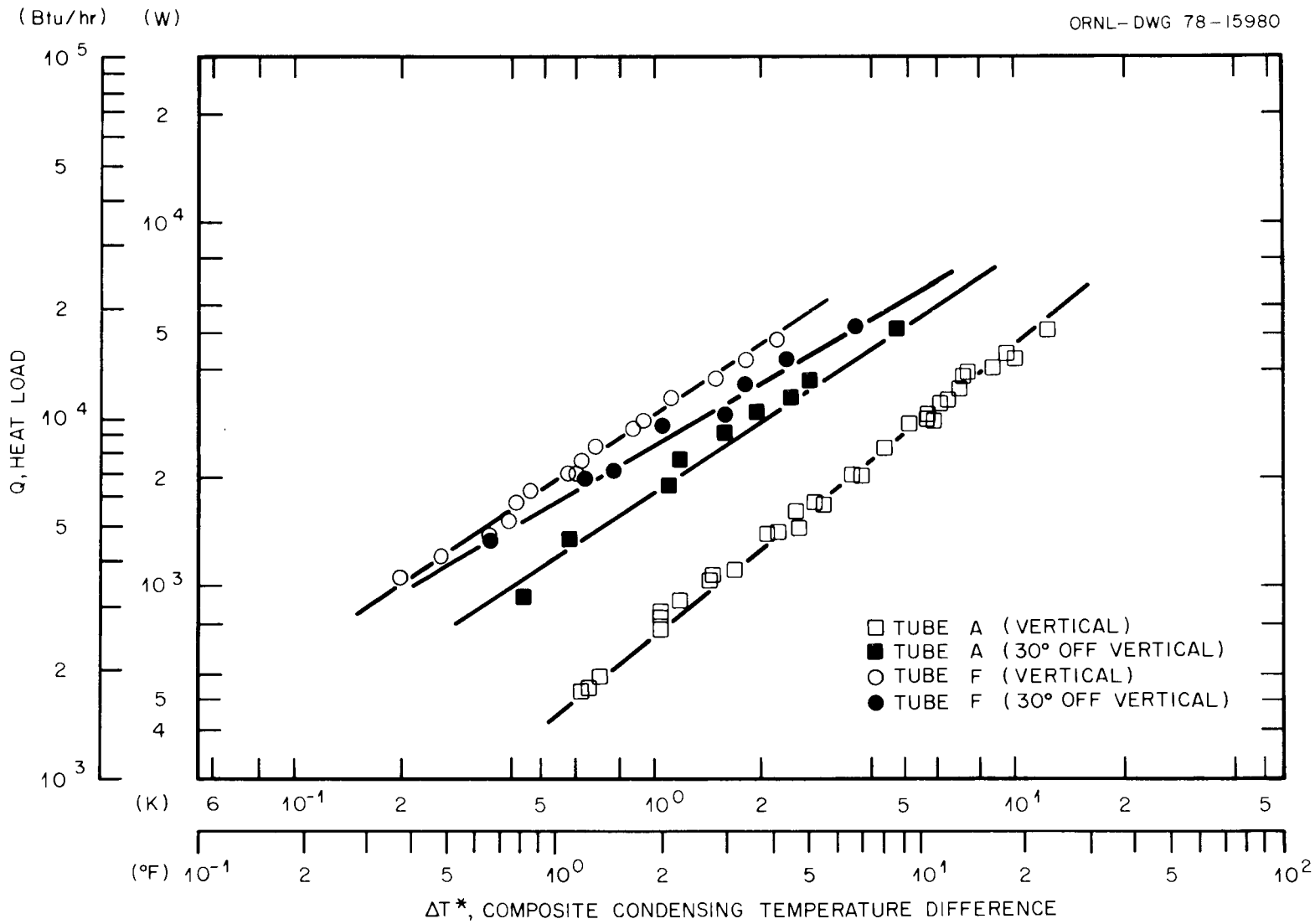

Fig. 5-4. Comparison of heat transfer performance of a smooth and a fluted tube for vertical and 30° off vertical orientations — Q vs ΔT*.

transfer performance of the fluted tube decreased slightly upon going to the inclined orientation as shown in Figs. 5-3 and 5-4.

The results for the inclined tests are not surprising. By inclining the smooth tube, the condensate is allowed to drain (or drip) along the entire length of the tube; whereas, for the vertical tube, all of the condensate exits at the bottom of the tube. This results in decreasing the "effective" thickness (or resistance) of the condensate film, thus, increasing the heat transfer coefficient at a given heat flux.

Hassan and Jakob[8] presented an analytical and experimental treatment for pure saturated vapors condensing on inclined circular cyclinders. The study contained some experimental data for steam condensing on inclined tubes; however, the deviation of the experimental data from those obtained analytically was quite large with the experimental film coefficients 28 to 100% higher than those predicted by the analysis. The authors suggested that more comprehensive experimental data were necessary for adequate modeling.

For the fluted tubes, the flutes served as the primary mode of film removal from the crests along the periphery before flowing down the tube in the troughs. Inclining the tube, apparently, decreases the overall efficiency of condensate removal resulting in a slightly greater "effective" film thickness, thus, a lower film heat transfer coefficient. An analytical model to describe this physical operation would be very complicated if at all possible, expecially, considering the difficulties for the simplier case of the smooth tube.

Doubly Fluted Tube

A doubly fluted tube (H) was tested in order to determine the effect of water velocity on the overall heat transfer performance of a tube with inside flutes. The data for ammonia condensing on tube H (42 outside and 34 inside flutes) are plotted in Figs. 5-5 and 5-6 in the form of heat load versus overall mean temperature difference. Figure 5-5 presents data taken with a 0.5-in.-diam rod installed through the inside of the test tube, and Fig. 5-6 presents data without the rod in place. As expected, the heat transfer performance of tube H with the rod

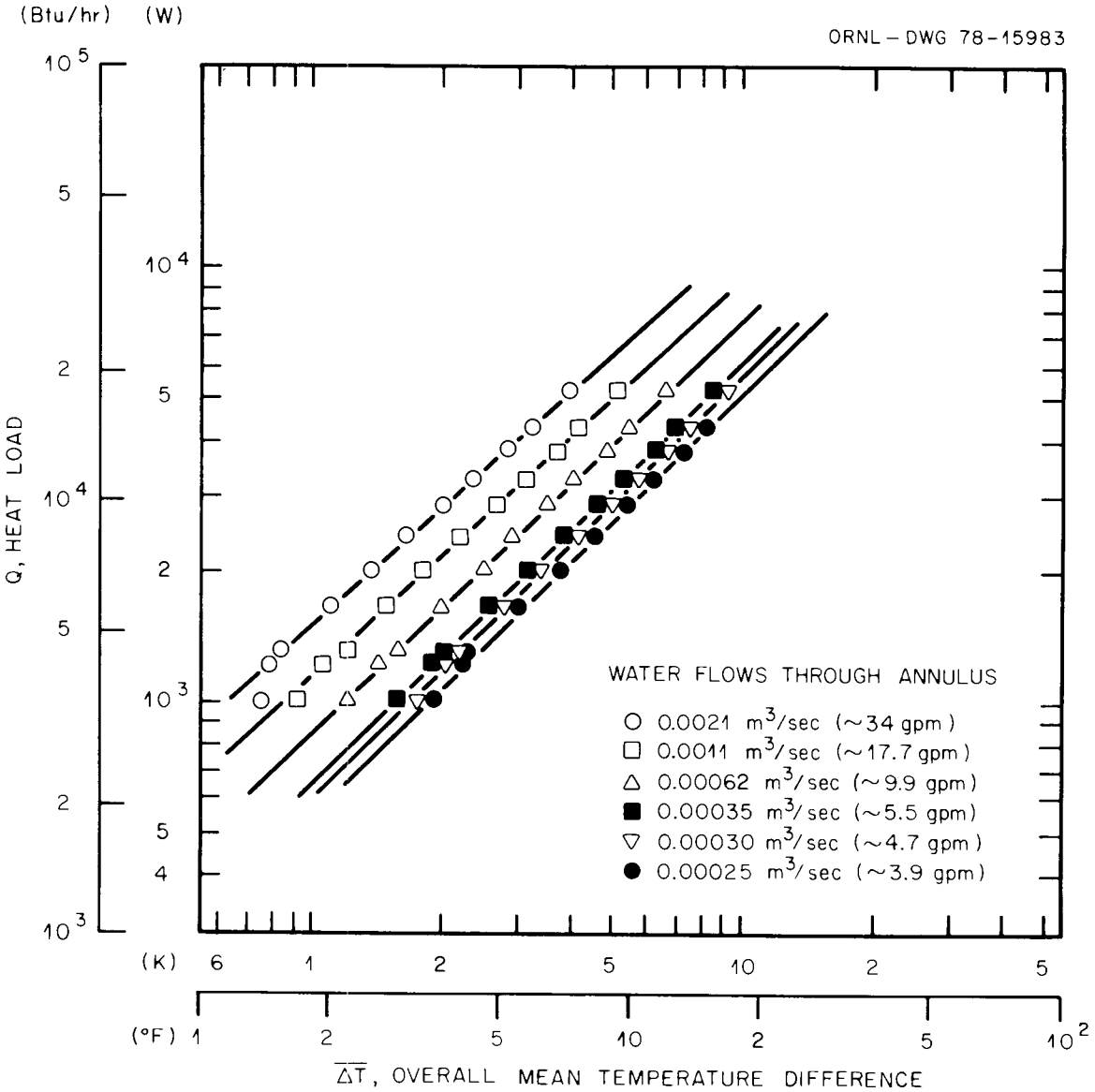

Fig. 5-5. Heat transfer performance of tube H [1.2 m (4-ft) long, 42 outside and 34 inside flutes] — ammonia condensing on the outside surface and water flowing through an annulus inside the tube.

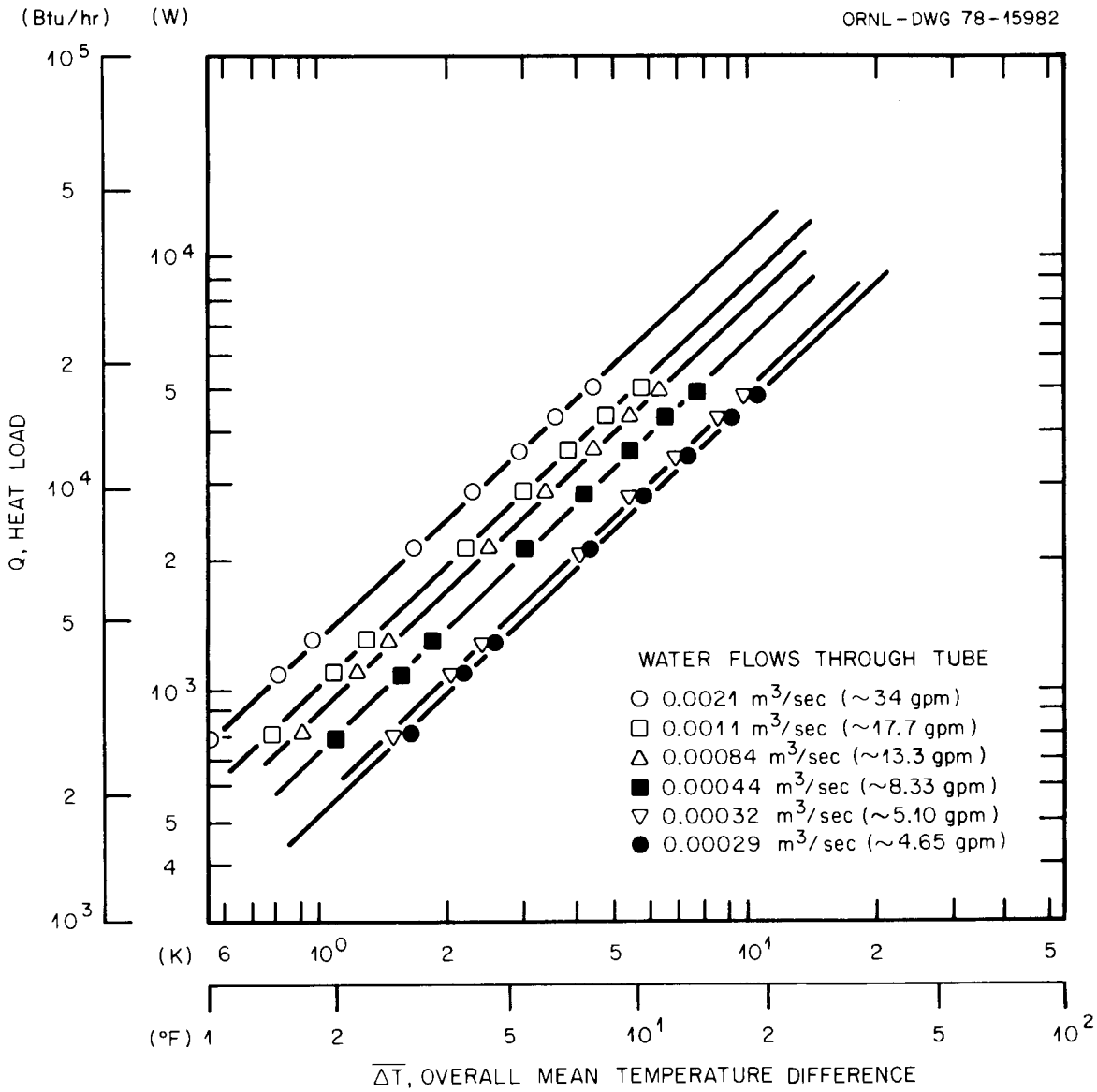

Fig. 5-6. Heat transfer performance of tube [1.2 m (4-ft) long, 42 outside and 34 inside flutes] — ammonia condensing on the outside surface and water flowing through the inside of the tube (no rod inside the tube).

installed is slightly better than that without the rod due to higher water-side heat transfer coefficients at the same water flow rate. This translates to smaller overall mean temperature differences at the same heat load and water flow rates.

For tube H, unlike other tubes tested with ammonia, the inside flutes result in water-side heat transfer enhancement. Therefore, the water-side coefficient is probably not a simple function of water velocity as assumed for the Wilson plot. Thus, the applicability of the Wilson plot for the analysis of this data is uncertain; and results with this method are not presented herein. Only overall heat transfer results are given (see Appendix C, Tables C-4 and C-5).

SUMMARY

The experimental data presented in this report add to previous heat transfer data taken at ORNL for condensation on vertical fluted tubes (for example, see Refs. 1, 2, and 3). For the range of heat fluxes tested, the results for the fluted tubes with drainage skirts indicated that the flutes were not near the flooding state; however, flooding should become more pronounced at higher heat fluxes where the liquid films are thicker. Thus, ammonia condensation data at higher heat fluxes would be useful in determining where shorter condensing lengths offer an advantage.

The results for the inclined smooth tube showed that considerable heat transfer enhancement can be achieved by simply inclining the condenser. The limiting case of this is the horizontal orientation. However, in the design of practical multitube condensers, it is necessary to consider interaction of tubes since condensate will drain from tube to tube. In contrast to smooth tubes, inclining of a fluted tube actually caused degradation in the heat transfer performance. More data are needed at various angles of inclination and for different tube geometries before any quantitative conclusions can be reached about this effect.

The data for the doubly fluted tube were the first ammonia data taken at ORNL in which the inside tube surface was also fluted. This resulted in an enhancement in the water-side heat transfer coefficient over that of an internally smooth tube at a given water flow rate; and thus, an increase in overall coefficient over that for a hypothetical tube with identical outside flutes and a smooth inside surface. This increase in water-side coefficient is an advantage over the singly fluted tubes.

REFERENCES

1. S. K. Combs, An Experimental Study of Heat Transfer Enhancement for Ammonia Condensing on Vertical Fluted Tubes, ORNL-5356 (January 1978).

2. S. K. Combs, G. S. Mailen, and R. W. Murphy, Condensation of Refrigerants on Vertical Fluted Tubes, ORNL/TM-5848 (August 1978).

3. L. G. Alexander and H. W. Hoffman, Improved Heat-Transfer Systems for Evaporators – Performance Characteristics of Advanced Evaporator Tubes for Long-Tube Vertical Evaporators, ORNL/TM-2951 (January 1971).

4. E. E. Wilson, "Basis for Rational Design of Heat Transfer Apparatus," *Trans. Am. Soc. Mech. Engrs.*, 37, 47 (1915).

5. "Properties of Refrigerants," Chap. 14, ASHRAE Handbook of Fundamentals, p. 268, ASHRAE, New York, 1972.

6. Thermophysical Properties of Refrigerants, pp. 145–150, ASHRAE, New York, 1973.

7. Thermodynamic Properties of Refrigerants, pp. 131–150, ASHRAE, New York, 1969.

8. K. E. Hassan and M. Jakob, "Laminar Film Condensation of Pure Saturated Vapors on Inclined Circular Cylinders," *Trans. Am. Soc. Mech. Engrs.*, 80, 887 (1958).

APPENDIX A

SAMPLES OF DATA REDUCTION

Physical Properties for Ammonia

All property data for ammonia used in data reduction were taken from ASHRAE handbooks[5-7] where ammonia is designated as R-717. The accuracy of thermophysical properties is discussed in Ref. 6.

Fluted Tube

A sample of the experimental data required for computing the heat transfer rates and coefficients in the condenser is listed in Table A-1. The data are for ammonia condensing on tube E (60 square ridges). The data were presented in the previous report;[1] however, the method of analysis is the same for all tubes. Experimental Run 717-051E is used to demonstrate the procedure followed in reducing the data for an individual run, and the series of Runs 717-051E through 717-056E are used to demonstrate the Wilson plot.

For saturated vapor, the experimental pressure (P) of the vapor should agree with the saturation pressure (P_{sat}) of ammonia at the experimental vapor temperature (T_v). The saturation pressure in ASHRAE for a temperature of 77.2°F is 146 psia which agrees within the experimental accuracy of the instruments to the measured pressure (P) of 147 psia for Run 717-051E. This agreement also indicates that noncondensables were not present in the condenser in appreciable amounts during operation.

The heat transfer rate in the condenser can be computed both from condensate flow rate (F_c) and from the flow rate (F_w) and the temperature rise (ΔT_w) of the cooling water. To calculate the heat transfer from the condensate flow rate requires the latent heat (h_{fg}) of ammonia at the vapor temperature (T_v) and the density of liquid ammonia (ρ_c) at the temperature of the condensate (T_c) at the measuring station.

Table A-1. Sample of experimental data — ammonia condensing on Tube E

Run No.	Vapor feed to test section		Condensate		Primary cooling water through test section			
	Temperature T_v, °F	Pressure P, psia	Flow rate F_c, gpm	Temperature T_c, °F	Flow rate F_w, gpm	Inlet temp. $T_{w,in}$, °F	Outlet temp. $T_{w,out}$, °F	Temp. dif.[a] ΔT_w, °F
717-051E	77.16	147.2	0.03114	77.16	33.4	75.27	75.62	0.284
717-052E	78.39	150.2	0.03119	78.14	17.7	75.64	76.22	0.570
716-053E	78.96	151.7	0.03096	78.68	9.55	74.77	75.78	1.01
717-054E	79.84	154.2	0.03105	79.40	7.70	74.92	76.16	1.23
717-055E	82.02	159.7	0.03082	81.22	5.10	75.30	77.13	1.83
717-056E	82.69	161.7	0.03119	81.82	4.65	75.38	77.40	2.02

[a]Corrected for temperature offset of instruments and pressure drop effects.

For

$$T_c = 77.2°F \qquad \rho_c = 37.6\ lb_m/ft^3$$

$$T_v = 77.2°F \qquad h_{fg} = 502\ Btu/lb_m$$

The heat transfer rate can be calculated from Eq. (4-2) with the condensate mass flow rate given by:

$$\dot{m}_c = F_c\ \rho_c\ , \tag{A-1}$$

so that

$$Q_c = F_c\ \rho_c\ h_{fg} \tag{A-2}$$

$$= (0.03114\ gpm)(37.6\ lb_m/ft^3)(502\ Btu/lb_m)(1\ ft^3/7.481\ gal)(60\ min/hr)$$

$$= 4710\ Btu/hr.$$

The heat transfer rate also can be computed from the primary cooling water and is given by Eq. (4-3) where

$$\dot{m}_w = F_w\ \rho_w\ ; \tag{A-3}$$

and therefore,

$$Q_w = F_w\ \rho_w\ c_{pw}\ \Delta T_w\ , \tag{A-4}$$

where c_{pw} and ρ_w are the heat capacity and density of the primary cooling water, respectively. These values are calculated at the average temperature of the primary cooling water. In this particular example, the change in temperature is so small that the variation in properties is insignificant. The properties for water in this range ($\sim$75°F) is a density (ρ_w) of 62.2 lb_m/ft^3 and a heat capacity (c_{pw}) of 1.0 $Btu/lb_m \cdot °F$. With the information for Run 717-051E,

$$Q_w = (33.4\ gpm)(62.2\ lb_m/ft^3)(1.0\ Btu/lb_m \cdot °F)(0.284°F)(1\ ft^3/7.481\ gal)$$

$$(60\ min/hr) = 4730\ Btu/hr\ .$$

The percent difference between the two heat loads is given by:

$$(\Delta Q/Q)\ X\ 100 = (Q_w - Q_c)/Q_c X\ 100 \tag{A-5}$$

$$= (4730 - 4710)/4710\ X\ 100$$

$$= 0.4\ .$$

The heat balance obtained by the two different methods thus agreed within acceptable limits.

The overall condensing coefficient can be computed from Eq. (4-5) with either Q_c or Q_w. However, since the heat rate from the condensate flow (Q_c) is considered the more accurate of the two, it is used in the calculation. The mean temperature difference ($\overline{\Delta T}$) is given by Eq. (4-4):

$$\overline{\Delta T} = T_v - (T_{w,in} + T_{w,out})/2 \ , \tag{4-4}$$

and for Run 717-051E,

$$\overline{\Delta T} = 77.16 - (75.27 + 75.62)/2 = 1.71°F \ .$$

The outside surface area (A_o) of tube E is listed in Ref. 1 (Table 2-1, p. 8). Applying Eq. (4-5) and using the data for Run 717-051E,

$$U_o = \frac{Q}{A_o \ \overline{\Delta T}} = \frac{4710 \text{ Btu/hr}}{(1.60 \text{ ft}^2)(1.71°F)} = 1720 \text{ Btu/hr}\cdot\text{ft}^2\cdot°F \ . \tag{4-5}$$

The same calculations illustrated for Run 717-051E can be carried out for the other five runs in Table A-1. The results of the calculations for all six runs are shown in Table A-2. The six heat rates can be averaged to obtain a mean heat load for the series of runs, so that

$$Q_{c,avg} = 4700 \text{ Btu/hr} \ ,$$

$$Q_{w,avg} = 4800 \text{ Btu/hr} \ .$$

Water velocities (v) are calculated from the volume flows of water (F_w) and the cross-sectional area of the annulus (A_c):

$$v = F_w/A_c \ , \tag{A-6}$$

and A_c is given by:

$$A_c = \pi D_i^2/4 - \pi D_r^2/4 \ , \tag{A-7}$$

where D_i is the inside diameter of the test tube and D_r is the outside diameter of the solid rod inserted through the test tube (D_r = 0.5 in.). From Ref. 1 (Table 2-1, p. 8) for tube E, D_i = 0.87 in., so that

$$A_c = \pi(0.87/12 \text{ ft})^2/4 - \pi(0.50/12 \text{ ft})^2/4 = 0.00276 \text{ ft}^2$$

and for Run 717-051E,

$$v = (33.4 \text{ gpm})\left(\frac{1 \text{ ft}^3}{7.481 \text{ gal}}\right)\left(\frac{1 \text{ min}}{60 \text{ sec}}\right)\Big/ 0.00276 \text{ ft}^2 = 26.9 \text{ ft/sec} \ .$$

Table A-2. Sample information for the Wilson plot — ammonia condensing on Tube E

Run No.	Condenser heat load			Condenser mean temp. diff., $\overline{\Delta T}$, °F	Primary cooling water velocity, v, ft/sec	$(1/v)^{0.8}$	Overall coefficient, U_o, Btu/hr·ft^2·°F	$1/U_o$
	Q_c,[a] Btu/hr	Q_w,[b] Btu/hr	$(\Delta Q/Q) \times 100$					
717-051E	4710	4730	0.4	1.71	26.9	7.18×10^{-2}	1720	5.81×10^{-4}
717-052E	4700	5030	7.0	2.47	14.3	1.19×10^{-1}	1190	8.40×10^{-4}
717-053E	4660	4810	3.3	3.69	7.70	1.95×10^{-1}	790	1.27×10^{-3}
717-054E	4660	4740	1.7	4.30	6.20	2.32×10^{-1}	670	1.49×10^{-3}
717-055E	4590	4650	1.3	5.80	4.11	3.23×10^{-1}	490	2.04×10^{-3}
717-056E	4640	4690	1.1	6.30	3.75	3.47×10^{-1}	460	2.17×10^{-3}

[a]Calculated from condensate flow of ammonia.

[b]Calculated from temperature rise and flow of the primary cooling water.

To generate the Wilson plot, it is necessary to take the reciprocal of the overall coefficient and to raise the water velocity to the negative 0.8 power. These values are shown in Table A-2 and were used to construct the Wilson plot shown in Fig. A-1. The data points shown in Fig. A-1 were fitted by a least-squares method of the first order to determine the best linear fit to satisfy the following relationship:

$$1/U_o = a_o + a_1 v^{-0.8} , \tag{4-9}$$

where a_1 is the slope of the straight line and a_o is the y-intercept. For this particular run series,

$$a_o = 1.51 \times 10^{-4} ,$$

$$a_1 = 5.81 \times 10^{-3} .$$

As indicated in Fig. A-1, the data show good linearity and allow extrapolation to infinite water velocity (zero water-side resistance) with some confidence. The reciprocal ($1/a_o$ or h^*) gives the composite heat transfer coefficient of the condensing film and wall. For the series of Runs 717-051E through 717-056E, the composite coefficient is 6600 Btu/hr·ft^2·°F as shown in Fig. A-1. The corresponding composite temperature difference is given by Eq. (4-14):

$$\Delta T^* = \frac{Q}{h^* A_o} = \frac{4700 \text{ Btu/hr}}{(6600 \text{ Btu/hr}\cdot\text{ft}^2\cdot{}^\circ\text{F})(1.60 \text{ ft}^2)} = 0.4^\circ\text{F} . \tag{4-14}$$

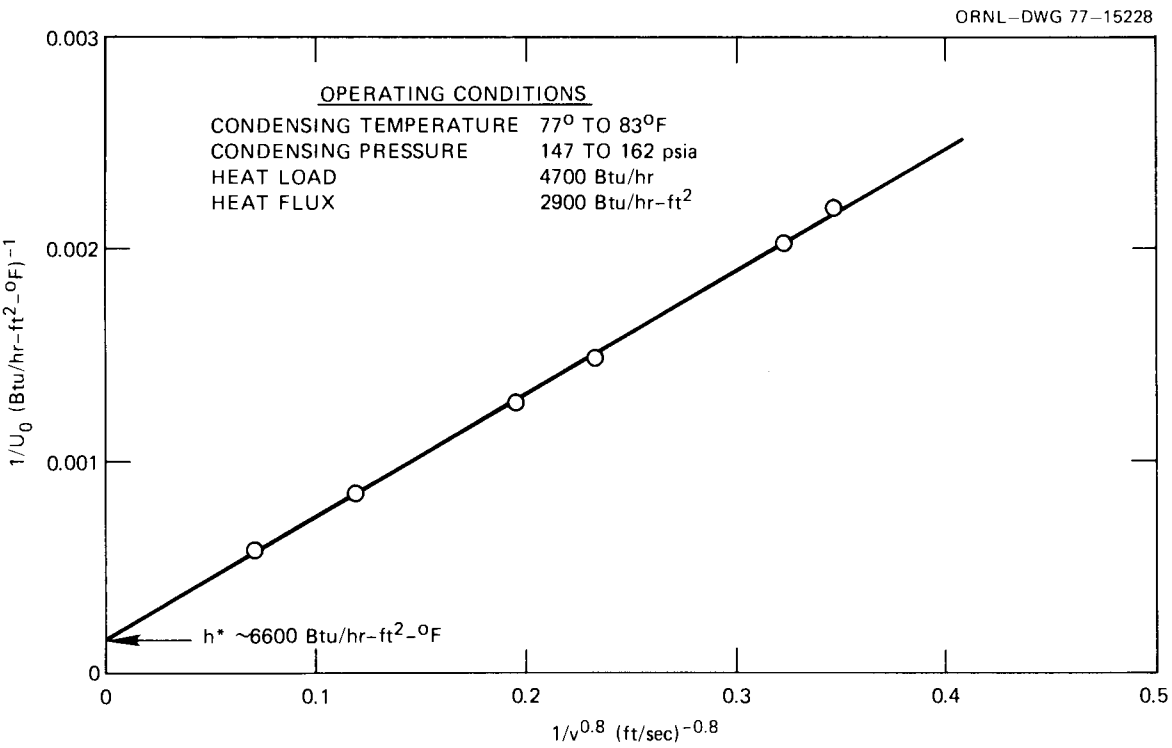

Fig. A-1. Wilson plot for ammonia condensing on tube E (60 square ridges) — Runs 717-051E to 717-056E.

APPENDIX B

WILSON-PLOT RESULTS

Tables B-1 through B-3 summarize the experimental conditions for all series of runs used to construct Wilson plots. The results from the Wilson plots are also listed. The condenser heat load was taken as the average heat load based on the condensate flow ($Q_{c,avg}$) for a series of runs (see Appendix A for an example). Individual runs are documented in detail in Appendix C.

Table B-1. Summary of experimental conditions and results from Wilson plots for ammonia condensing on tube F-7 (a duplicate of tube F with 7 skirts)

Series of runs	Condenser heat load		Condensing temperature range		Condensing heat transfer coefficient, h*		Condensing temperature difference, ΔT*	
	W	(Btu/hr)	K	(°F)	$W/m^2 \cdot K$	$(Btu/hr \cdot ft^2 \cdot °F)$	K	(°F)
717-030F7 to 035F7	2400	(8300)	300–306	(80–91)	35,000	(6100)	0.7	(1.3)
717-036F7 to 041F7	2000	(6900)	303–307	(85–94)	34,000	(6800)	0.6	(1.0)
717-042F7 to 047F7	3500	(11900)	304–312	(87-103)	30,000	(5200)	1.2	(2.2)
717-048F7 to 053F7	1300	(4600)	303–306	(85–91)	40,000	(7000)	0.3	(0.6)
717-054F7 to 057F7	5000	(16900)	304–312	(88–102)	26,000	(4600)	2.0	(3.6)
717-048F7 to 063F7	1700	(5900)	304–308	(87–95)	36,000	(6300)	0.5	(0.9)
717-064F7 to 069F7	2800	(9700)	304–312	(87–102)	36,000	(6300)	0.8	(1.5)
717-070F7 to 074F7	1100	(3700)	303–305	(85-89)	45,000	(8000)	0.2	(0.4)
716-075F7 to 080F7	4100	(13900)	304–310	(87–99)	30,000	(5300)	1.4	(2.5)

Table B-2. Summary of experimental conditions and results from Wilson plots for ammonia condensing on tube AT (smooth tube 30° off vertical)

Series of runs	Condenser heat load		Condensing temperature range		Condensing heat transfer coefficient, h*		Condensing temperature difference, ΔT*	
	W	(Btu/hr)	K	(°F)	$W/m^2 \cdot K$	$(Btu/hr \cdot ft^2 \cdot °F)$	K	(°F)
717-001AT to 006AT	3300	(11200)	304–314	(88–105)	14,000	(2400)	2.5	(4.5)
717-007AT to 010AT	5100	(17300)	306–317	(91–110)	11,000	(1900)	4.9	(8.9)
717-012AT to 017AT	2200	(7600)	302–309	(84–96)	19,000	(3300)	1.2	(2.2)
717-018AT to 023AT	1300	(4500)	303–307	(85–92)	22,000	(3900)	0.6	(1.1)
717-024AT to 029AT	2600	(8800)	302–308	(83–95)	16,000	(2800)	1.6	(3.0)
717-030AT to 035AT	1800	(6100)	302–307	(84–92)	16,000	(2800)	1.2	(2.1)
717-036AT to 040AT	910	(3100)	300–303	(81–85)	20,000	(3600)	0.4	(0.8)
717-041AT to 046AT	3700	(12800)	304–311	(88–100)	14,000	(2400)	2.8	(5.1)
717-047AT to 052AT	3000	(10200)	305–314	(89–104)	15,000	(2700)	2.0	(3.6)

Table B-3. Summary of experimental conditions and results from Wilson plots for ammonia condensing on tube FT (F 30° off vertical)

Series of runs	Condenser heat load		Condensing temperature range		Condensing heat transfer coefficient, h*		Condensing temperature difference, ΔT*	
	W	(Btu/hr)	K	(°F)	$W/m^2 \cdot K$	$(Btu/hr \cdot ft^2 \cdot °F)$	K	(°F)
717-001FT to 006FT	2900	(9900)	303–310	(85–98)	18,000	(3200)	1.7	(3.0)
717-007FT to 012FT	2000	(6900)	304–309	(87–97)	26,000	(4600)	0.8	(1.5)
717-013FT to 018FT	1300	(4500)	302–306	(84–91)	37,000	(6600)	0.4	(0.7)
717-019FT to 024FT	3700	(12500)	303–312	(85–101)	20,000	(3600)	1.8	(3.3)
717-025FT to 030FT	2000	(6800)	302–307	(84–93)	31,000	(5400)	0.6	(1.2)
717-031FT to 036FT	2800	(9700)	303–310	(85–99)	27,000	(4700)	1.1	(2.0)
717-042FT to 046FT	5000	(17100)	302–314	(84–106)	14,000	(2400)	3.8	(6.8)
717-047FT to 052FT	4200	(14500)	302–313	(83–104)	18,000	(3200)	2.4	(4.4)

APPENDIX C

EXPERIMENTAL DATA

Tables C-1 through C-5 document 501 runs which yielded 92 data points or Wilson plots. The tables summarize the experimental data used in data reduction. In addition, the tables list saturation pressures and heat balance checks. Velocities are presented along with Reynolds number for the water flows. Also, overall heat transfer coefficients are tabulated. The information was generated by a computer code used for data reduction, and the runs are grouped in series corresponding to Wilson plots. Several series of runs were discarded because of problems with operation and/or instrumentation. An average inside diameter for tube H was estimated as 0.88 in. to allow calculation of water velocities through the tube.

Table C-1. Experimental data for ammonia condensing on tube F-7 (a duplicate of tube F with 7 skirts)

Run No.	T_v, °F	P, psia	P_{sat}, psia	F_c, gpm	T_c, °F	$\dot{m}_c$, lb_m/hr	F_w, gpm	v, ft/sec	Re	$T_{w,in}$, °F	$T_{w,out}$, °F	ΔT_w, °F	$\overline{\Delta T}$, °F	Q_c, Btu/hr	Q_w, Btu/hr	$\frac{\Delta Q}{Q}$ X 100	U_o, $\frac{Btu}{hr \cdot ft^2 \cdot °F}$
R-717-030F7	79.48	152.7	151.7	0.0558	79.21	16.79	34.0	24.8	84342.	75.61	76.18	0.50	3.58	8381.	8430.	0.6	2252.
R-717-031F7	80.69	155.7	154.8	0.0564	80.25	16.94	17.7	12.9	43787.	75.20	76.17	0.96	5.01	8432.	8494.	0.7	1622.
R-717-032F7	83.51	163.2	162.3	0.0563	82.79	16.88	9.5	6.9	23656.	75.29	77.10	1.81	7.32	8353.	8587.	2.8	1100.
R-717-033F7	87.65	174.7	173.8	0.0542	86.38	16.14	4.8	3.5	12061.	74.92	78.22	3.34	11.08	7919.	8038.	1.5	689.
R-717-034F7	87.71	175.2	174.0	0.0565	86.52	16.84	5.2	3.8	13089.	75.13	78.35	3.25	10.97	8265.	8471.	2.5	726.
R-717-035F7	91.05	184.7	183.7	0.0570	89.41	16.90	3.8	2.8	9739.	75.29	79.56	4.29	13.62	8233.	8241.	0.1	582.
R-717-036F7	84.81	167.7	165.9	0.0471	83.58	14.10	34.0	24.8	91094.	81.80	82.26	0.39	2.78	6961.	6632.	-4.7	2410.
R-717-037F7	86.46	171.2	170.5	0.0475	85.05	14.17	17.7	12.9	47690.	82.08	82.90	0.82	3.96	6971.	7232.	3.7	1694.
R-717-038F7	88.26	177.2	175.6	0.0476	86.54	14.17	9.8	7.2	26593.	81.95	83.37	1.42	5.60	6943.	6997.	0.8	1194.
R-717-039F7	91.52	186.2	185.2	0.0476	89.31	14.13	5.3	3.9	14456.	81.74	84.33	2.64	8.49	6876.	7012.	2.0	780.
R-717-040F7	92.58	189.7	188.3	0.0478	90.33	14.18	4.7	3.4	12768.	81.68	84.64	3.00	9.42	6883.	7029.	2.1	704.
R-717-041F7	93.86	193.7	192.2	0.0478	91.41	14.15	4.0	2.9	10999.	81.65	85.04	3.41	10.52	6853.	6879.	0.4	628.
R-717-042F7	86.63	172.2	171.0	0.0821	85.70	24.48	34.0	24.8	90365.	80.98	81.77	0.72	5.25	12041.	12229.	1.6	2208.
R-717-043F7	89.69	180.2	179.7	0.0827	88.56	24.56	17.7	12.9	47580.	81.59	83.01	1.41	7.39	12001.	12477.	4.0	1565.
R-717-044F7	93.28	191.2	190.5	0.0831	91.92	24.56	9.8	7.2	26711.	81.79	84.25	2.46	10.26	11910.	12113.	1.7	1118.
R-717-045F7	98.96	209.7	208.5	0.0839	97.18	24.59	5.4	3.9	14710.	81.45	85.94	4.53	15.27	11773.	12169.	3.4	743.
R-717-046F7	100.84	214.7	214.7	0.0843	98.84	24.67	4.7	3.4	12922.	81.61	86.71	5.14	16.68	11759.	12052.	2.5	679.
R-717-047F7	103.23	223.7	222.8	0.0851	101.18	24.80	4.0	2.9	11056.	81.61	87.59	6.00	18.63	11756.	11977.	1.9	608.
R-717-048F7	85.10	168.7	166.7	0.0319	84.16	9.55	34.0	24.8	92514.	83.12	83.48	0.28	1.80	4712.	4834.	2.6	2524.
R-717-049F7	85.64	169.2	168.2	0.0318	84.66	9.50	17.7	12.9	48019.	82.79	83.33	0.53	2.59	4682.	4724.	0.9	1744.
R-717-050F7	86.85	172.7	171.6	0.0315	85.47	9.39	9.8	7.2	26752.	82.66	83.63	0.97	3.71	4617.	4761.	3.1	1199.
R-717-051F7	88.58	177.7	176.5	0.0317	86.91	9.44	5.5	4.0	15057.	82.21	83.90	1.73	5.52	4625.	4793.	3.6	807.
R-717-052F7	89.52	179.7	179.2	0.0319	87.75	9.47	4.7	3.4	12794.	82.34	84.32	2.01	6.19	4630.	4724.	2.0	721.
R-717-053F7	90.49	182.7	182.1	0.0316	88.48	9.39	4.0	2.9	10928.	82.49	84.77	2.30	6.86	4582.	4586.	0.1	643.
R-717-054F7	88.13	176.7	175.2	0.1179	87.57	35.06	34.0	24.8	88738.	79.36	80.47	1.04	8.22	17186.	17674.	2.8	2013.
R-717-055F7	96.70	202.2	201.1	0.1197	95.77	35.17	9.9	7.2	26223.	79.63	83.23	3.61	15.27	16922.	17742.	4.8	1068.
R-717-056F7	106.03	232.7	232.6	0.1224	104.33	35.51	5.5	4.0	15030.	80.43	86.87	6.47	22.38	16724.	17766.	6.2	720.
R-717-057F7	101.86	217.7	218.1	0.1216	100.45	35.49	7.0	5.1	18876.	80.01	85.11	5.12	19.30	16879.	17893.	6.0	843.
R-717-058F7	87.38	174.7	173.1	0.0407	86.02	12.12	34.0	24.8	94539.	84.89	85.29	0.33	2.28	5951.	5631.	-5.4	2511.
R-717-059F7	88.63	177.7	176.6	0.0410	87.05	12.20	18.5	13.5	51600.	85.01	85.70	0.68	3.27	5975.	6294.	5.3	1758.
R-717-060F7	90.25	182.7	181.4	0.0410	88.50	12.19	9.7	7.1	27193.	84.91	86.13	1.23	4.73	5948.	5965.	0.3	1211.
R-717-061F7	92.53	189.7	188.2	0.0406	90.31	12.03	5.4	4.0	15254.	84.58	86.71	2.16	6.89	5842.	5875.	0.6	817.
R-717-062F7	93.42	191.7	190.9	0.0413	91.18	12.21	4.8	3.5	13368.	84.53	86.97	2.48	7.67	5918.	5913.	-0.1	743.
R-717-063F7	94.58	195.7	194.5	0.0412	92.07	12.17	3.9	2.9	11024.	84.36	87.30	2.96	8.75	5882.	5805.	-1.3	648.
R-717-064F7	88.56	177.7	176.5	0.0669	87.51	19.89	34.0	24.8	93957.	84.26	84.90	0.56	3.99	9741.	9583.	-1.6	2355.
R-717-065F7	89.99	181.7	180.6	0.0665	88.78	19.75	18.4	13.4	50823.	84.00	85.08	1.07	5.46	9647.	9867.	2.3	1704.
R-717-066F7	93.09	191.2	189.9	0.0672	91.46	19.89	9.8	7.1	27316.	84.32	86.28	1.96	7.80	9645.	9607.	-0.4	1192.
R-717-067F7	97.51	205.2	203.7	0.0679	95.53	19.97	5.4	3.9	15157.	84.11	87.65	3.58	11.63	9593.	9639.	0.5	795.
R-717-068F7	99.92	212.7	211.6	0.0689	97.75	20.18	4.6	3.4	13145.	84.54	88.69	4.19	13.30	9640.	9699.	0.6	698.
R-717-069F7	101.56	217.7	217.1	0.0692	99.34	20.24	4.0	2.9	11262.	84.28	89.13	4.87	14.86	9633.	9654.	0.2	624.

Table C-1 (continued)

Run No.	T_v, °F	P, psia	P_{sat}, psia	F_c, gpm	T_c, °F	$\dot{m}_c$, lb_m/hr	F_w, gpm	v, ft/sec	Re	$T_{w,in}$, °F	$T_{w,out}$, °F	ΔT_w, °F	$\overline{\Delta T}$, °F	Q_c, Btu/hr	Q_w, Btu/hr	$\frac{\Delta Q}{Q}$ X 100	U_o, $\frac{Btu}{hr \cdot ft^2 \cdot °F}$
R-717-070F7	85.07	168.2	166.6	0.0251	83.69	7.52	34.0	24.8	92945.	83.53	83.83	0.23	1.39	3709.	3969.	7.0	2576.
R-717-071F7	85.79	169.7	168.6	0.0253	84.17	7.57	17.5	12.8	47875.	83.52	83.97	0.45	2.04	3729.	3920.	5.1	1760.
R-717-072F7	86.60	172.2	170.9	0.0251	84.87	7.50	9.8	7.1	26654.	83.30	84.07	0.78	2.92	3691.	3779.	2.4	1218.
R-717-073F7	88.41	177.2	176.0	0.0251	86.28	7.49	5.5	4.0	15169.	83.45	84.78	1.37	4.29	3670.	3784.	3.1	823.
R-717-074F7	88.75	178.2	177.0	0.0245	86.68	7.29	4.8	3.5	13170.	83.22	84.75	1.58	4.76	3569.	3776.	5.8	722.
R-717-075F7	87.42	174.2	173.2	0.0966	86.65	28.76	34.0	24.8	90164.	80.74	81.65	0.85	6.22	14120.	14349.	1.6	2185.
R-717-076F7	89.64	180.7	179.6	0.0969	88.74	28.78	18.4	13.4	48782.	80.37	81.98	1.60	8.47	14065.	14732.	4.7	1600.
R-717-077F7	93.73	193.2	191.9	0.0978	92.57	28.87	9.8	7.2	26286.	80.27	83.15	2.88	12.03	13982.	14171.	1.4	1120.
R-717-078F7	102.30	219.7	219.6	0.0989	100.24	28.88	4.5	3.3	12065.	78.99	85.19	6.25	20.21	13721.	14024.	2.2	654.
R-717-079F7	101.19	216.7	215.8	0.0993	99.22	29.02	4.9	3.6	13064.	79.09	84.84	5.79	19.22	13822.	14105.	2.0	693.
R-717-080F7	99.36	211.2	209.8	0.0988	97.62	28.96	5.5	4.0	14649.	79.00	84.10	5.12	17.81	13855.	14040.	1.3	749.

Table C-2. Experimental data for ammonia condensing on tube AT (tube A — 30° off vertical)

Run No.	T_v, °F	P, psia	P_{sat}, psia	F_c, gpm	T_c, °F	$\dot{m}_c$, lb_m/hr	F_w, gpm	v, ft/sec	Re	$T_{w,in}$, °F	$T_{w,out}$, °F	ΔT_w, °F	$\overline{\Delta T}$, °F	Q_c, Btu/hr	Q_w, Btu/hr	$\frac{\Delta Q}{Q} \times 100$	U_o, $\frac{Btu}{hr \cdot ft^2 \cdot °F}$
R-717-001AT	87.81	175.2	174.3	0.0776	86.84	23.10	17.7	14.3	45898.	77.01	78.33	1.31	10.14	11332.	11585.	2.2	1067.
R-717-002AT	91.84	187.2	186.1	0.0785	90.82	23.23	9.5	7.7	24714.	76.70	79.15	2.45	13.91	11297.	11606.	2.7	775.
R-717-003AT	97.17	203.7	202.6	0.0785	95.22	23.09	5.4	4.4	14267.	76.35	80.49	4.13	18.74	11100.	11234.	1.2	566.
R-717-004AT	99.38	210.7	209.8	0.0789	97.14	23.15	4.7	3.8	12358.	76.37	81.19	4.81	20.60	11072.	11285.	1.9	513.
R-717-005AT	105.30	229.7	230.0	0.0803	102.61	23.35	3.3	2.6	8627.	76.06	83.00	6.94	25.77	11016.	11252.	2.1	408.
R-717-006AT	90.57	179.7	182.3	0.1213	88.47	36.04	34.4	27.7	87482.	75.58	76.71	1.06	14.43	17579.	18225.	3.7	1164.
R-717-007AT	95.44	195.2	197.2	0.1227	93.26	36.21	17.7	14.3	44956.	74.99	77.11	2.11	19.40	17471.	18666.	6.8	860.
R-717-008AT	102.32	218.2	219.7	0.1244	99.92	36.32	9.8	7.9	25484.	75.61	79.37	3.77	24.83	17257.	18505.	7.2	664.
R-717-009AT	107.02	234.7	236.1	0.1261	104.37	36.59	7.6	6.1	20067.	76.48	81.32	4.85	28.12	17194.	18452.	7.3	584.
R-717-010AT	109.93	244.7	246.8	0.1277	107.09	36.89	6.3	5.1	16558.	75.92	81.81	5.93	31.06	17215.	18614.	8.1	529.
R-717-012AT	83.96	164.2	163.6	0.0516	82.49	15.47	34.4	27.7	91587.	79.51	80.04	0.46	4.19	7652.	7928.	3.6	1744.
R-717-013AT	85.99	169.2	169.1	0.0523	84.23	15.63	17.7	14.3	47200.	79.44	80.35	0.90	6.09	7696.	7956.	3.4	1207.
R-717-014AT	88.77	177.7	177.0	0.0518	86.69	15.44	9.8	7.9	26327.	79.69	81.29	1.60	8.28	7557.	7832.	3.6	872.
R-717-015AT	92.75	189.7	188.9	0.0526	90.17	15.59	5.4	4.4	14754.	79.73	82.50	2.81	11.64	7569.	7645.	1.0	621.
R-717-016AT	94.07	193.7	192.9	0.0529	91.35	15.65	4.7	3.8	12820.	79.59	82.82	3.27	12.86	7574.	7718.	1.9	563.
R-717-017AT	95.59	198.7	197.6	0.0531	92.61	15.69	4.0	3.2	10872.	79.56	83.33	3.79	14.15	7568.	7563.	-0.1	511.
R-717-018AT	84.67	166.2	165.5	0.0310	82.00	9.28	34.4	27.7	94637.	82.25	82.60	0.28	2.25	4584.	4736.	3.3	1946.
R-717-019AT	86.54	171.2	170.7	0.0310	83.72	9.26	17.7	14.3	49185.	82.99	83.50	0.51	3.30	4555.	4494.	-1.3	1319.
R-717-020AT	88.04	175.7	175.0	0.0312	85.04	9.30	9.8	7.9	27428.	82.95	83.89	0.95	4.63	4560.	4653.	2.0	941.
R-717-021AT	90.04	181.2	180.8	0.0311	86.62	9.26	5.5	4.5	15480.	82.73	84.38	1.68	6.49	4523.	4662.	3.1	666.
R-717-022AT	90.96	183.7	183.5	0.0313	87.49	9.31	4.6	3.7	12822.	82.70	84.66	1.97	7.28	4536.	4515.	-0.4	595.
R-717-023AT	91.74	185.7	185.8	0.0312	88.04	9.28	4.0	3.2	11179.	82.60	84.84	2.26	8.02	4515.	4514.	-0.0	538.
R-717-024AT	82.47	159.7	159.5	0.0604	81.05	18.12	34.4	27.7	88774.	76.79	77.79	0.53	5.17	8991.	9078.	1.0	1660.
R-717-025AT	84.98	166.7	166.4	0.0603	83.07	18.04	17.7	14.3	45856.	77.08	78.12	1.02	7.38	8905.	9051.	1.6	1152.
R-717-026AT	87.71	174.2	174.0	0.0607	85.84	18.10	10.0	8.1	25950.	76.84	78.63	1.79	9.98	8881.	8930.	0.6	850.
R-717-027AT	92.43	188.7	187.9	0.0612	89.84	18.13	5.3	4.3	13894.	76.57	79.90	3.36	14.19	8807.	8928.	1.4	593.
R-717-028AT	93.63	191.7	191.5	0.0611	91.02	18.07	4.7	3.8	12398.	76.50	80.21	3.73	15.27	8756.	8818.	0.7	548.
R-717-029AT	95.01	196.7	195.8	0.0611	92.06	18.06	4.0	3.2	10465.	76.23	80.53	4.32	16.63	8723.	8624.	-1.1	501.
R-717-030AT	83.66	162.2	162.7	0.0415	81.05	12.47	34.4	27.7	91716.	79.67	80.10	0.36	3.78	6169.	6247.	1.3	1561.
R-717-031AT	84.80	166.2	165.9	0.0419	82.40	12.56	17.7	14.3	47236.	79.59	80.33	0.73	4.84	6199.	6419.	3.6	1223.
R-717-032AT	87.08	172.7	172.2	0.0420	84.25	12.55	9.8	7.9	26477.	79.89	81.19	1.30	6.54	6167.	6378.	3.4	901.
R-717-033AT	89.90	180.7	180.3	0.0421	86.80	12.53	5.6	4.5	14994.	79.70	81.90	2.24	9.09	6121.	6213.	1.5	643.
R-717-034AT	90.95	183.7	183.4	0.0421	87.65	12.53	4.8	3.8	12830.	79.65	82.21	2.57	10.02	6107.	6099.	-0.1	582.
R-717-035AT	92.29	187.7	187.5	0.0423	88.81	12.57	4.0	3.2	10831.	79.62	82.65	3.05	11.16	6106.	6090.	-0.3	523.
R-717-036AT	80.51	155.2	154.4	0.0208	77.01	6.28	17.7	14.3	46227.	78.04	78.43	0.38	2.28	3129.	3373.	7.8	1313.
R-717-037AT	81.81	158.2	157.8	0.0207	77.75	6.25	9.9	8.0	26131.	78.36	79.00	0.65	3.13	3103.	3251.	4.8	948.
R-717-038AT	83.18	162.2	161.4	0.0207	78.76	6.24	5.5	4.5	14582.	78.14	79.29	1.19	4.47	3090.	3289.	6.4	661.
R-717-039AT	83.80	163.7	163.1	0.0206	79.39	6.20	4.7	3.8	12302.	78.08	79.42	1.36	5.05	3069.	3184.	3.8	581.
R-717-040AT	84.65	165.7	165.4	0.0217	79.93	6.51	3.9	3.1	10230.	77.96	79.61	1.67	5.86	3217.	3243.	0.8	524.

Table C-2 (continued)

Run No.	T_v, °F	P, psia	P_{sat}, psia	F_c, gpm	T_c, °F	$\dot{m}_c$, lb_m/hr	F_w, gpm	v, ft/sec	Re	$T_{w,in}$, °F	$T_{w,out}$, °F	ΔT_w, °F	$\overline{\Delta T}$, °F	Q_c, Btu/hr	Q_w, Btu/hr	$\frac{\Delta Q}{\overline{Q}} \times 100$	U_o, $\frac{Btu}{hr \cdot ft^2 \cdot °F}$
R-717-041AT	88.15	175.2	175.3	0.0882	86.13	26.30	34.4	27.7	91740.	79.49	80.31	0.75	8.25	12892.	12922.	0.2	1493.
R-717-042AT	91.71	184.7	185.7	0.0893	89.13	26.50	17.7	14.3	47144.	79.04	80.57	1.52	11.90	12893.	13466.	4.4	1034.
R-717-043AT	96.75	200.7	201.3	0.0904	94.19	26.62	9.9	8.0	26885.	79.63	82.29	2.66	15.79	12808.	13218.	3.2	775.
R-717-044AT	102.32	219.7	219.7	0.0913	99.14	26.68	5.5	4.5	15068.	79.01	83.68	4.71	20.98	12677.	13041.	2.9	577.
R-717-045AT	105.59	230.7	231.0	0.0929	102.19	27.05	4.6	3.7	12574.	79.09	84.71	5.65	23.69	12752.	12959.	1.6	514.
R-717-046AT	99.58	209.7	210.5	0.0910	96.64	26.70	7.7	6.2	20922.	79.62	83.00	3.40	18.27	12765.	13085.	2.5	667.
R-717-047AT	88.50	176.7	176.3	0.0704	86.60	20.97	34.4	27.7	94492.	81.96	82.64	0.61	6.21	10274.	10417.	1.4	1581.
R-717-048AT	91.18	184.2	184.1	0.0706	89.06	20.97	17.7	14.3	48721.	81.87	83.07	1.19	8.71	10213.	10525.	3.1	1120.
R-717-049AT	95.23	197.2	196.5	0.0717	92.69	21.17	9.8	7.9	27275.	82.29	84.46	2.17	11.85	10222.	10628.	4.0	824.
R-717-050AT	99.86	212.7	211.4	0.0723	97.00	21.20	5.4	4.4	15220.	81.76	85.55	3.83	16.20	10130.	10413.	2.8	597.
R-717-051AT	102.22	219.7	219.3	0.0732	99.15	21.39	4.7	3.8	13211.	82.16	86.59	4.45	17.84	10165.	10409.	2.4	544.
R-717-052AT	104.19	227.2	226.1	0.0733	101.01	21.38	4.0	3.2	11200.	82.13	87.29	5.17	19.48	10116.	10223.	1.1	496.

Table C-3. Experimental data for ammonia condensing on tube FT (tube F – 30° off vertical)

Run No.	T_v, °F	P, psia	P_{sat}, psia	F_c, gpm	T_c, °F	$\dot{m}_c$, lb_m/hr	F_w, gpm	v, ft/sec	Re	$T_{w,in}$, °F	$T_{w,out}$, °F	ΔT_w, °F	$\overline{\Delta T}$, °F	Q_c, Btu/hr	Q_w, Btu/hr	$\frac{\Delta Q}{Q} \times 100$	U_o, $\frac{Btu}{hr \cdot ft^2 \cdot °F}$
R-717-001FT	85.21	165.7	167.0	0.0678	81.34	20.34	34.4	25.1	89674.	79.48	80.15	0.60	5.40	10033.	10314.	2.8	1791.
R-717-002FT	86.99	170.2	172.0	0.0682	82.99	20.43	17.7	12.9	46095.	79.15	80.33	1.17	7.25	10042.	10349.	3.1	1334.
R-717-003FT	90.35	179.7	181.7	0.0685	86.12	20.41	9.8	7.1	25801.	79.67	81.72	2.06	9.65	9958.	10051.	0.9	994.
R-717-004FT	95.41	196.2	197.1	0.0681	90.87	20.16	5.0	3.7	13398.	79.43	83.35	3.96	14.02	9729.	9962.	2.4	669.
R-717-005FT	96.31	198.7	199.9	0.0687	91.68	20.30	4.7	3.5	12641.	79.57	83.74	4.21	14.65	9778.	9953.	1.8	643.
R-717-006FT	98.12	205.7	205.7	0.0692	93.51	20.41	4.0	2.9	10590.	79.41	84.35	4.96	16.25	9791.	9800.	0.1	581.
R-717-007FT	86.94	172.2	171.8	0.0470	83.25	14.06	34.5	25.2	94580.	83.68	84.15	0.40	3.03	6909.	6919.	0.1	2200.
R-717-008FT	89.16	177.7	178.2	0.0476	85.31	14.21	17.7	12.9	49025.	84.36	85.18	0.81	4.39	6952.	7179.	3.3	1527.
R-717-009FT	91.46	184.2	185.0	0.0480	87.35	14.27	9.8	7.1	27314.	84.58	86.00	1.42	6.17	6945.	6952.	0.1	1085.
R-717-010FT	94.44	194.2	194.0	0.0476	89.77	14.12	5.2	3.8	14547.	84.29	86.91	2.66	8.84	6828.	6908.	1.2	744.
R-717-011FT	95.55	197.7	197.5	0.0487	91.16	14.41	4.8	3.5	13324.	84.38	87.29	2.95	9.72	6951.	6995.	0.6	689.
R-717-012FT	96.87	201.7	201.7	0.0491	92.23	14.50	4.0	2.9	11179.	84.21	87.68	3.49	10.92	6973.	6931.	-0.6	615.
R-717-013FT	84.45	165.7	164.9	0.0306	80.07	9.20	34.5	25.2	93167.	82.52	82.84	0.25	1.77	4543.	4337.	-4.5	2471.
R-717-014FT	85.48	168.7	167.7	0.0308	81.00	9.24	17.7	12.9	47944.	82.66	83.19	0.52	2.56	4555.	4574.	0.4	1716.
R-717-015FT	86.97	172.2	171.9	0.0310	82.29	9.29	9.8	7.2	26785.	82.79	83.71	0.93	3.73	4567.	4565.	-0.0	1181.
R-717-016FT	89.60	179.7	179.5	0.0312	84.32	9.31	5.3	3.9	14529.	83.05	84.77	1.75	5.69	4550.	4638.	1.9	771.
R-717-017FT	90.53	182.7	182.2	0.0311	85.20	9.27	4.6	3.3	12553.	83.29	85.24	1.99	6.26	4521.	4531.	0.2	695.
R-717-018FT	91.21	184.7	184.2	0.0312	85.88	9.29	3.9	2.9	10823.	83.18	85.41	2.25	6.92	4524.	4417.	-2.4	630.
R-717-019FT	85.14	167.2	166.8	0.0862	83.00	25.82	34.5	25.2	88441.	78.08	78.88	0.73	6.66	12738.	12633.	-0.8	1842.
R-717-020FT	86.66	171.2	171.0	0.0860	84.12	25.70	17.7	12.9	45109.	77.28	78.75	1.46	8.65	12637.	12856.	1.7	1408.
R-717-021FT	90.43	182.7	181.9	0.0865	87.54	25.74	9.8	7.2	25276.	77.25	79.87	2.63	11.87	12556.	12918.	2.9	1019.
R-717-022FT	96.51	201.2	200.5	0.0870	92.94	25.67	5.3	3.9	13598.	76.92	81.68	4.80	17.21	12358.	12569.	1.7	692.
R-717-023FT	98.14	206.7	205.8	0.0879	94.53	25.88	4.7	3.4	12198.	76.78	82.14	5.40	18.68	12416.	12661.	2.0	640.
R-717-024FT	101.13	215.7	215.6	0.0885	97.28	25.94	3.9	2.9	10300.	77.11	83.39	6.31	20.88	12359.	12363.	0.0	570.
R-717-025FT	83.80	163.7	163.1	0.0462	80.45	13.89	34.5	25.2	91095.	80.63	81.07	0.38	2.95	6871.	6471.	-5.8	2245.
R-717-026FT	84.86	166.7	166.0	0.0466	81.43	14.00	17.7	12.9	46710.	80.41	81.20	0.78	4.05	6909.	6931.	0.3	1642.
R-717-027FT	86.94	172.2	171.8	0.0464	83.21	13.89	9.8	7.2	26099.	80.43	81.83	1.40	5.81	6827.	6869.	0.6	1131.
R-717-028FT	89.82	180.7	180.1	0.0466	85.49	13.90	5.4	4.0	14477.	80.11	82.56	2.49	8.49	6791.	6770.	-0.3	771.
R-717-029FT	91.10	184.7	183.9	0.0470	86.77	13.99	4.7	3.4	12490.	80.09	82.99	2.93	9.56	6813.	6862.	0.7	687.
R-717-030FT	92.91	190.2	189.3	0.0471	88.30	13.98	3.9	2.9	10556.	80.55	83.93	3.40	10.67	6786.	6668.	-1.7	613.
R-717-031FT	85.33	167.7	167.3	0.0661	83.13	19.80	34.4	25.1	90795.	80.50	81.13	0.57	4.51	9764.	9747.	-0.2	2086.
R-717-032FT	87.66	174.7	173.9	0.0667	85.33	19.90	17.7	12.9	47143.	81.00	82.10	1.10	6.11	9767.	9704.	-0.6	1539.
R-717-033FT	90.82	183.7	183.0	0.0672	88.25	19.96	9.8	7.1	26143.	81.09	83.11	2.03	8.72	9729.	9854.	1.3	1075.
R-717-034FT	95.50	197.7	197.3	0.0676	92.35	19.98	5.4	3.9	14530.	81.02	84.66	3.67	12.66	9639.	9842.	2.1	734.
R-717-035FT	97.02	202.7	202.2	0.0680	93.90	20.03	4.7	3.4	12749.	81.15	85.28	4.17	13.80	9631.	9754.	1.3	672.
R-717-036FT	98.96	209.2	208.5	0.0683	95.61	20.07	4.0	2.9	10907.	81.06	85.89	4.84	15.49	9610.	9666.	0.6	598.
R-717-042FT	84.17	164.7	164.1	0.1178	79.73	35.42	34.5	25.2	81763.	71.82	72.98	1.09	11.77	17510.	18725.	6.9	1433.
R-717-043FT	87.86	174.7	174.4	0.1179	83.25	35.29	17.7	12.9	42348.	72.10	74.14	2.04	14.74	17310.	18057.	4.3	1131.
R-717-044FT	94.67	195.2	194.8	0.1199	89.86	35.53	9.9	7.3	24480.	73.43	77.08	3.66	19.41	17175.	18157.	5.7	852.
R-717-045FT	102.39	220.7	219.9	0.1208	96.98	35.45	5.5	4.0	13840.	73.12	79.49	6.40	26.08	16838.	17728.	5.3	622.
R-717-046FT	106.24	233.7	233.3	0.1225	100.88	35.73	4.7	3.4	11844.	73.34	80.91	7.62	29.12	16819.	17864.	6.2	557.
R-717-047FT	83.00	161.7	161.0	0.0980	79.75	29.49	34.5	25.2	84281.	74.25	75.17	0.85	8.29	14612.	14698.	0.6	1698.
R-717-048FT	85.24	167.7	167.1	0.0996	81.86	29.86	17.7	12.9	42958.	73.35	75.07	1.72	11.03	14728.	15187.	3.1	1286.
R-717-049FT	90.53	182.7	182.2	0.1001	86.50	29.83	9.8	7.2	24434.	74.38	77.41	3.04	14.63	14549.	14918.	2.5	958.
R-717-050FT	98.16	206.7	205.8	0.1026	93.76	30.24	5.5	4.0	13903.	74.67	80.07	5.45	20.79	14505.	14942.	3.0	672.
R-717-051FT	100.69	214.7	214.2	0.1033	96.33	30.33	4.7	3.4	11975.	74.50	80.81	6.35	23.04	14465.	14950.	3.3	605.
R-717-052FT	103.84	225.2	224.9	0.1038	99.28	30.33	4.0	2.9	10159.	74.63	82.04	7.42	25.50	14361.	14699.	2.4	542.

Table C-4. Experimental data for ammonia condensing on tube H (0.5-in.-OD rod on water side)

Run No.	T_v, °F	P, psia	P_{sat}, psia	F_c, gpm	T_c, °F	$\dot{m}_c$, lb_m/hr	F_w, gpm	v, ft/sec	Re	$T_{w,in}$, °F	$T_{w,out}$, °F	ΔT_w, °F	$\overline{\Delta T}$, °F	Q_c, Btu/hr	Q_w, Btu/hr	$\frac{\Delta Q}{Q} \times 100$	U_o, $\frac{Btu}{hr \cdot ft^2 \cdot °F}$
R-717-001H	85.71	169.2	168.4	0.0387	85.24	11.54	34.0	27.4	44142.	83.50	83.90	0.33	2.01	5687.	5614.	-1.3	1607.
R-717-002H	87.05	172.7	172.1	0.0387	86.41	11.54	17.1	13.8	22371.	83.99	84.68	0.69	2.71	5669.	5920.	4.4	1187.
R-717-003H	88.01	175.2	174.9	0.0390	87.23	11.61	9.8	7.9	12902.	83.85	85.02	1.18	3.58	5691.	5818.	2.2	904.
R-717-004H	89.52	179.7	179.2	0.0388	88.49	11.53	5.5	4.5	7292.	83.81	85.87	2.08	4.68	5636.	5762.	2.2	684.
R-717-005H	90.12	181.7	181.0	0.0389	89.00	11.53	4.7	3.8	6173.	83.79	86.24	2.48	5.11	5631.	5797.	2.9	626.
R-717-006H	90.64	183.2	182.5	0.0388	89.29	11.52	4.0	3.2	5253.	83.65	86.50	2.88	5.56	5616.	5728.	2.0	574.
R-717-007H	86.75	171.7	171.3	0.0773	86.29	23.03	34.0	27.4	43486.	82.09	82.85	0.69	4.28	11323.	11720.	3.5	1503.
R-717-008H	88.32	176.7	175.7	0.0776	87.92	23.07	17.4	14.0	22303.	81.97	83.33	1.34	5.67	11304.	11675.	3.3	1133.
R-717-009H	90.83	184.2	183.1	0.0777	90.12	23.03	10.0	8.1	12956.	82.38	84.68	2.30	7.30	11228.	11499.	2.4	874.
R-717-010H	94.80	196.7	195.1	0.0790	93.90	23.28	5.5	4.5	7308.	83.10	87.26	4.20	9.62	11248.	11589.	3.0	664.
R-717-011H	96.05	199.7	199.1	0.0791	95.04	23.26	4.7	3.8	6218.	83.18	88.06	4.92	10.43	11211.	11491.	2.5	611.
R-717-012H	97.05	203.7	202.3	0.0789	96.02	23.18	4.0	3.2	5298.	82.95	88.61	5.69	11.28	11144.	11289.	1.3	562.
R-717-013H	89.09	179.2	178.0	0.1255	88.85	37.27	33.3	26.8	42275.	81.28	82.45	1.10	7.23	18236.	18257.	0.1	1433.
R-717-014H	90.93	184.7	183.4	0.1253	90.49	37.12	17.7	14.3	22419.	80.63	82.73	2.10	9.25	18089.	18534.	2.5	1111.
R-717-015H	94.88	196.7	195.4	0.1271	94.22	37.43	9.8	7.9	12654.	80.96	84.71	3.76	12.05	18084.	18481.	2.2	853.
R-717-016H	100.59	213.7	213.8	0.1290	99.60	37.68	5.5	4.5	7323.	81.74	88.35	6.65	15.55	17973.	18420.	2.5	657.
R-717-017H	102.82	221.7	221.4	0.1311	101.61	38.18	4.7	3.8	6244.	82.07	89.87	7.84	16.85	18118.	18313.	1.1	611.
R-717-018H	86.87	172.2	171.6	0.0312	85.46	9.32	34.0	27.4	45007.	85.15	85.48	0.26	1.55	4581.	4461.	-2.6	1675.
R-717-019H	88.18	175.7	175.4	0.0313	86.67	9.32	17.7	14.3	23593.	85.75	86.31	0.55	2.15	4566.	4840.	6.0	1206.
R-717-020H	89.14	178.2	178.1	0.0311	87.55	9.26	9.9	8.0	13303.	85.82	86.75	0.93	2.85	4531.	4614.	1.8	902.
R-717-021H	90.15	181.2	181.1	0.0311	88.44	9.24	5.5	4.5	7436.	85.64	87.29	1.69	3.69	4510.	4672.	3.6	694.
R-717-022H	90.70	183.2	182.7	0.0310	89.14	9.20	4.7	3.8	6289.	85.75	87.66	1.95	4.00	4486.	4550.	1.4	638.
R-717-023H	91.34	185.2	184.6	0.0307	89.74	9.11	3.9	3.1	5255.	85.81	88.07	2.28	4.40	4437.	4438.	0.0	573.
R-717-024H	88.10	175.2	175.1	0.0570	87.24	16.97	34.0	27.4	44874.	84.78	85.35	0.50	3.04	8319.	8532.	2.6	1556.
R-717-025H	89.39	179.2	178.9	0.0577	88.37	17.14	18.4	14.8	24381.	84.92	85.87	0.94	4.00	8381.	8638.	3.1	1192.
R-717-026H	91.86	186.7	186.1	0.0578	90.60	17.13	9.8	7.9	13205.	85.67	87.36	1.70	5.34	8329.	8350.	0.2	886.
R-717-027H	93.94	193.2	192.5	0.0579	92.53	17.10	5.4	4.4	7345.	85.42	88.49	3.11	6.99	8281.	8436.	1.9	673.
R-717-028H	94.81	196.2	195.2	0.0580	93.37	17.10	4.7	3.8	6360.	85.54	89.08	3.58	7.51	8261.	8390.	1.6	625.
R-717-029H	95.90	199.2	198.6	0.0585	94.33	17.23	3.9	3.2	5339.	85.54	89.74	4.23	8.26	8306.	8272.	-0.4	571.
R-717-030H	87.75	174.2	174.1	0.0676	87.03	20.13	34.0	27.4	44320.	83.71	84.36	0.58	3.72	9876.	9905.	0.3	1509.
R-717-031H	89.25	178.7	178.4	0.0682	88.37	20.26	17.7	14.3	23168.	83.81	84.95	1.14	4.87	9911.	10066.	1.6	1156.
R-717-032H	91.61	186.2	185.4	0.0687	90.61	20.33	9.9	8.0	13105.	84.22	86.24	2.02	6.38	9894.	9981.	0.9	881.
R-717-033H	94.62	195.2	194.6	0.0686	93.40	20.24	5.4	4.4	7287.	84.49	88.10	3.66	8.32	9783.	9929.	1.5	668.
R-717-034H	95.32	197.7	196.8	0.0686	94.13	20.21	4.7	3.8	6275.	84.25	88.44	4.23	8.97	9757.	9890.	1.4	618.
R-717-035H	96.55	201.2	200.7	0.0689	95.20	20.27	3.9	3.2	5281.	84.22	89.19	4.99	9.84	9759.	9763.	0.0	563.
R-717-036H	86.38	170.7	170.2	0.0470	85.72	14.00	34.0	27.4	44212.	83.60	84.07	0.40	2.55	6891.	6801.	-1.3	1536.
R-717-037H	87.48	173.7	173.4	0.0472	86.75	14.06	18.5	14.9	24150.	83.76	84.54	0.77	3.33	6904.	7125.	3.2	1179.
R-717-038H	89.45	179.2	179.0	0.0475	88.61	14.11	9.8	7.9	12989.	84.29	85.70	1.41	4.46	6896.	6938.	0.6	878.
R-717-039H	91.21	185.2	184.2	0.0474	90.30	14.03	5.4	4.3	7154.	84.11	86.66	2.59	5.82	6834.	6982.	2.2	667.
R-717-040H	91.69	186.2	185.7	0.0472	90.77	13.98	4.7	3.8	6206.	84.00	86.93	2.97	6.23	6802.	6932.	1.9	621.
R-717-041H	92.85	190.2	189.2	0.0478	91.82	14.13	3.9	3.2	5243.	84.24	87.71	3.49	6.88	6859.	6850.	-0.1	566.

Table C-4 (continued)

Run No.	T_v, °F	P, psia	P_{sat}, psia	F_c, gpm	T_c, °F	$\dot{m}_c$, lb_m/hr	F_w, gpm	v, ft/sec	Re	$T_{w,in}$, °F	$T_{w,out}$, °F	ΔT_w, °F	$\overline{\Delta T}$, °F	Q_c, Btu/hr	Q_w, Btu/hr	$\frac{\Delta Q}{Q}$ X 100	U_o, $\frac{Btu}{hr \cdot ft^2 \cdot °F}$
R-717-042H	86.02	169.2	169.2	0.0899	85.78	26.80	34.0	27.4	42627.	80.42	81.28	0.79	5.17	13196.	13349.	1.2	1451.
R-717-043H	87.89	174.7	174.5	0.0905	87.48	26.92	17.7	14.3	22274.	80.37	81.93	1.55	6.74	13204.	13713.	3.9	1113.
R-717-044H	90.85	183.7	183.1	0.0912	90.26	27.03	9.8	7.9	12535.	80.70	83.42	2.72	8.79	13177.	13385.	1.6	852.
R-717-045H	94.85	196.2	195.3	0.0918	93.97	27.05	5.4	4.4	7057.	81.05	85.91	4.91	11.37	13069.	13338.	2.1	653.
R-717-046H	95.96	199.2	198.8	0.0922	94.97	27.14	4.7	3.8	6077.	80.88	86.54	5.70	12.24	13081.	13312.	1.8	607.
R-717-047H	97.17	203.2	202.6	0.0917	96.11	26.93	3.9	3.2	5111.	80.51	87.17	6.68	13.33	12947.	13090.	1.1	552.
R-717-048H	84.73	165.7	165.7	0.0239	83.85	7.13	34.0	27.4	43945.	83.19	83.48	0.22	1.40	3522.	3681.	4.5	1433.
R-717-049H	85.37	168.2	167.4	0.0240	84.52	7.18	17.7	14.3	22974.	83.46	83.90	0.43	1.69	3542.	3823.	8.0	1194.
R-717-050H	86.43	171.2	170.4	0.0238	85.53	7.10	9.8	7.9	12869.	83.86	84.59	0.73	2.20	3495.	3587.	2.6	901.
R-717-051H	87.15	173.2	172.4	0.0235	86.09	7.02	5.4	4.4	7119.	83.56	84.85	1.33	2.95	3447.	3630.	5.3	665.
R-717-052H	87.42	173.7	173.2	0.0231	86.31	6.89	4.6	3.7	6010.	83.46	85.00	1.57	3.19	3382.	3610.	6.7	602.
R-717-053H	87.85	175.2	174.4	0.0236	86.80	7.02	3.9	3.2	5142.	83.46	85.24	1.79	3.50	3444.	3519.	2.2	560.
R-717-054H	86.50	171.2	170.6	0.1017	86.16	30.31	34.0	27.4	42489.	80.11	81.07	0.90	5.91	14908.	15197.	1.9	1433.
R-717-055H	88.46	176.7	176.1	0.1019	87.96	30.29	17.7	14.3	22204.	80.03	81.76	1.72	7.56	14842.	15223.	2.6	1115.
R-717-056H	91.82	187.2	186.1	0.1030	91.22	30.47	9.8	7.9	12512.	80.37	83.45	3.08	9.91	14820.	15159.	2.3	849.
R-717-057H	96.10	200.2	199.2	0.1032	95.23	30.34	5.4	4.4	7049.	80.66	86.12	5.49	12.71	14620.	14940.	2.2	653.
R-717-058H	97.76	205.2	204.5	0.1040	96.71	30.51	4.7	3.8	6114.	80.89	87.20	6.34	13.71	14647.	14840.	1.3	607.
R-717-059H	99.90	212.7	211.5	0.1047	98.77	30.64	3.9	3.2	5177.	81.16	88.66	7.51	14.99	14638.	14733.	0.7	555.
R-717-060H	84.43	166.2	164.8	0.0288	83.68	8.61	34.0	27.4	43750.	82.81	83.12	0.24	1.47	4253.	4088.	-3.9	1647.
R-717-061H	85.11	167.7	166.7	0.0288	84.06	8.62	17.7	14.3	22832.	82.92	83.42	0.49	1.94	4251.	4362.	2.6	1244.
R-717-062H	85.90	169.7	168.9	0.0281	84.91	8.40	9.8	7.9	12726.	82.87	83.74	0.88	2.60	4138.	4304.	4.0	904.
R-717-063H	87.56	174.2	173.6	0.0287	86.22	8.56	5.5	4.4	7198.	83.30	84.84	1.58	3.49	4203.	4354.	3.6	685.
R-717-064H	88.09	176.2	175.1	0.0286	86.85	8.53	4.7	3.8	6138.	83.46	85.27	1.84	3.72	4182.	4314.	3.2	638.
R-717-065H	88.72	178.2	176.9	0.0286	87.32	8.51	3.9	3.2	5158.	83.54	85.67	2.14	4.11	4166.	4203.	0.9	576.
R-717-066H	86.90	172.7	171.7	0.1064	86.50	31.69	34.0	27.4	42563.	80.23	81.22	0.92	6.17	15577.	15689.	0.7	1434.
R-717-067H	88.61	177.2	176.6	0.1071	88.07	31.83	18.0	14.5	22521.	79.79	81.58	1.78	7.93	15590.	15957.	2.4	1117.
R-717-068H	92.62	189.7	188.4	0.1076	91.85	31.80	9.8	7.9	12569.	80.68	83.89	3.22	10.33	15443.	15808.	2.4	849.
R-717-069H	97.17	203.7	202.6	0.1080	96.19	31.72	5.4	4.4	7096.	81.10	86.78	5.72	13.23	15247.	15552.	2.0	655.
R-717-070H	98.59	208.7	207.2	0.1088	98.55	31.83	4.7	3.8	6165.	81.10	87.65	6.59	14.22	15251.	15482.	1.5	610.
R-717-071H	101.17	216.7	215.8	0.1090	100.00	31.84	3.9	3.2	5214.	81.57	89.43	7.88	15.67	15166.	15447.	1.9	550.

Table C-5. Experimental data for ammonia condensing on tube HN (tube H with no rod on water side)

Run No.	T_v, °F	P, psia	P_{sat}, psia	F_c, gpm	T_c, °F	$\dot{m}_c$, lb_m/hr	F_w, gpm	v, ft/sec	Re	$T_{w,in}$, °F	$T_{w,out}$, °F	ΔT_w, °F	$\overline{\Delta T}$, °F	Q_c, Btu/hr	Q_w, Btu/hr	$\frac{\Delta Q}{Q}$ X 100	U_o, $\frac{Btu}{hr \cdot ft^2 \cdot °F}$
R-717-001HN	83.75	164.7	163.0	0.0493	82.91	14.76	33.3	18.0	109122.	80.52	80.99	0.44	3.00	7304.	7276.	-0.4	1385.
R-717-002HN	84.10	164.7	163.9	0.0491	83.13	14.69	17.7	9.5	57570.	79.73	80.58	0.79	3.95	7262.	6949.	-4.3	1046.
R-717-003HN	84.39	165.7	164.7	0.0495	83.42	14.81	13.3	7.2	43105.	79.30	80.44	1.10	4.52	7317.	7305.	-0.2	919.
R-717-004HN	85.77	169.2	168.5	0.0491	84.58	14.67	8.3	4.5	27143.	79.43	81.17	1.71	5.47	7229.	7110.	-1.6	751.
R-717-005HN	88.27	176.7	175.6	0.0492	86.68	14.66	4.9	2.7	16214.	79.42	82.35	2.91	7.39	7183.	7161.	-0.3	553.
R-717-006HN	88.84	178.2	177.3	0.0497	87.20	14.78	4.6	2.5	15298.	79.49	82.66	3.14	7.77	7237.	7282.	0.6	529.
R-717-007HN	87.00	173.7	172.0	0.1173	86.32	34.97	33.3	18.0	106914.	78.57	79.66	1.05	7.89	17183.	17476.	1.7	1238.
R-717-008HN	89.68	180.7	179.7	0.1181	89.07	35.05	17.7	9.5	57095.	78.48	80.50	1.98	10.19	17126.	17510.	2.2	955.
R-717-009HN	91.74	186.7	185.8	0.1178	90.80	34.88	13.3	7.2	43389.	79.05	81.75	2.67	11.34	16967.	17695.	4.3	850.
R-717-010HN	95.05	196.7	195.9	0.1176	93.90	34.66	8.3	4.5	27294.	79.22	83.45	4.20	13.71	16741.	17315.	3.4	694.
R-717-011HN	100.10	213.2	212.2	0.1184	98.71	34.65	5.1	2.8	17063.	79.04	85.86	6.79	17.65	16545.	17275.	4.4	532.
R-717-012HN	101.77	217.7	217.8	0.1189	100.20	34.70	4.5	2.5	15279.	78.90	86.59	7.66	19.03	16509.	17378.	5.3	493.
R-717-013HN	83.41	162.7	162.1	0.0249	82.09	7.46	34.0	18.3	113059.	81.82	82.08	0.22	1.47	3693.	3816.	3.3	1430.
R-717-014HN	83.74	163.2	163.0	0.0252	82.30	7.54	17.7	9.5	58730.	81.54	82.00	0.42	1.97	3731.	3717.	-0.4	1075.
R-717-015HN	83.95	164.7	163.5	0.0252	82.46	7.54	13.3	7.2	44095.	81.41	82.00	0.55	2.24	3729.	3623.	-2.8	944.
R-717-016HN	84.87	166.7	166.0	0.0254	83.15	7.59	8.2	4.4	27155.	81.53	82.49	0.93	2.86	3746.	3786.	1.0	744.
R-717-017HN	86.21	169.7	169.8	0.0253	84.24	7.55	5.1	2.8	17072.	81.75	83.23	1.45	3.72	3716.	3689.	-0.7	568.
R-717-018HN	86.72	171.7	171.2	0.0252	84.50	7.52	4.6	2.5	15487.	81.96	83.60	1.61	3.94	3697.	3700.	0.1	533.
R-717-019HN	85.53	169.2	167.9	0.0669	84.72	19.98	17.7	9.5	57522.	79.53	80.65	1.08	5.44	9850.	9536.	-3.2	1029.
R-717-020HN	86.54	171.7	170.7	0.0668	85.72	19.91	13.3	7.2	43394.	79.67	81.15	1.43	6.14	9795.	9514.	-2.9	907.
R-717-021HN	88.43	177.2	176.1	0.0668	87.47	19.86	8.3	4.5	27344.	79.72	82.08	2.33	7.53	9731.	9678.	-0.5	734.
R-717-022HN	91.16	185.2	184.1	0.0665	89.81	19.73	5.1	2.8	16861.	79.58	83.37	3.76	9.69	9608.	9556.	-0.5	563.
R-717-023HN	92.16	188.2	187.1	0.0666	90.65	19.73	4.6	2.5	15356.	79.60	83.86	4.23	10.43	9589.	9761.	1.8	523.
R-717-024HN	85.43	166.2	167.6	0.0670	83.89	20.05	33.3	18.0	108394.	79.92	80.52	0.57	5.21	9885.	9469.	-4.2	1078.
R-717-025HN	86.22	170.7	169.8	0.0303	84.66	9.04	33.3	18.0	114176.	84.32	84.61	0.26	1.76	4449.	4402.	-1.0	1440.
R-717-026HN	86.91	172.7	171.7	0.0302	85.10	9.02	17.7	9.5	60776.	84.33	84.84	0.48	2.33	4432.	4212.	-5.0	1082.
R-717-027HN	87.36	173.7	173.0	0.0303	85.54	9.04	13.3	7.2	45738.	84.38	85.05	0.65	2.65	4438.	4299.	-3.1	952.
R-717-028HN	88.40	176.7	176.0	0.0306	86.42	9.13	8.3	4.5	28774.	84.54	85.63	1.05	3.31	4471.	4376.	-2.1	767.
R-717-029HN	89.72	180.7	179.8	0.0304	87.57	9.06	5.1	2.8	17674.	84.47	86.24	1.73	4.37	4424.	4409.	-0.3	575.
R-717-030HN	90.14	181.7	181.0	0.0306	87.99	9.09	4.6	2.5	16140.	84.51	86.46	1.91	4.65	4439.	4433.	-0.1	542.
R-717-031HN	86.46	171.7	170.5	0.0839	85.76	25.01	34.0	18.3	111959.	80.78	81.52	0.71	5.31	12303.	12127.	-1.4	1318.
R-717-032HN	88.17	175.2	175.3	0.0835	87.13	24.85	17.7	9.5	58410.	80.63	82.02	1.37	6.84	12180.	12079.	-0.8	1012.
R-717-033HN	89.45	179.2	179.0	0.0843	88.39	25.05	13.3	7.2	44068.	80.73	82.58	1.82	7.80	12247.	12109.	-1.1	892.
R-717-034HN	91.74	186.2	185.8	0.0842	90.42	24.95	8.4	4.6	28177.	80.79	83.75	2.93	9.47	12137.	12332.	1.6	728.
R-717-035HN	95.70	198.7	198.0	0.0843	94.08	24.84	5.1	2.8	17255.	80.95	85.78	4.81	12.33	11981.	12235.	2.1	552.
R-717-036HN	96.60	201.2	200.8	0.0846	94.81	24.90	4.6	2.5	15774.	80.96	86.21	5.22	13.02	11983.	12104.	1.0	523.
R-717-037HN	86.05	169.7	169.3	0.0999	85.25	29.83	33.3	18.0	107427.	79.02	79.97	0.92	6.55	14687.	15267.	3.9	1275.
R-717-038HN	88.24	175.7	175.5	0.1011	87.25	30.07	17.7	9.5	57239.	78.83	80.56	1.70	8.55	14740.	14984.	1.7	980.
R-717-039HN	89.53	179.7	179.3	0.1011	88.59	30.02	13.3	7.2	43115.	78.73	81.04	2.27	9.65	14672.	15074.	2.7	864.
R-717-040HN	92.51	188.7	188.1	0.1019	91.32	30.14	8.4	4.6	27715.	79.02	82.64	3.57	11.68	14640.	15053.	2.8	712.
R-717-041HN	97.78	205.2	204.6	0.1036	96.27	30.43	5.0	2.7	16546.	79.15	85.27	6.09	15.57	14608.	15066.	3.1	533.
R-717-042HN	98.86	208.7	208.1	0.1051	97.17	30.83	4.6	2.5	15565.	79.16	85.81	6.62	16.38	14762.	15363.	4.1	512.

Table C-5 (continued)

Run No.	T_v, °F	P, psia	P_{sat}, psia	F_c, gpm	T_c, °F	$\dot{m}_c$, lb_m/hr	F_w, gpm	v, ft/sec	Re	$T_{w,in}$, °F	$T_{w,out}$, °F	ΔT_w, °F	$\overline{\Delta T}$, °F	Q_c, Btu/hr	Q_w, Btu/hr	$\frac{\Delta Q}{Q}$ X 100	U_o, $\frac{Btu}{hr \cdot ft^2 \cdot °F}$
R-717-043HN	87.15	173.2	172.4	0.0676	86.34	20.14	33.3	18.0	112152.	82.68	83.30	0.59	4.16	9894.	9801.	-0.9	1350.
R-717-044HN	88.58	176.7	176.5	0.0675	87.52	20.09	17.7	9.5	59727.	82.58	83.71	1.09	5.43	9840.	9669.	-1.7	1029.
R-717-045HN	89.44	179.2	179.0	0.0676	88.36	20.10	13.3	7.2	44967.	82.57	84.04	1.43	6.13	9824.	9488.	-3.4	910.
R-717-046HN	91.69	186.2	185.7	0.0675	90.36	20.01	8.3	4.5	28447.	82.95	85.32	2.34	7.56	9735.	9711.	-0.2	732.
R-717-047HN	94.69	195.2	194.8	0.0680	93.02	20.07	5.2	2.8	17861.	83.03	86.84	3.78	9.75	9700.	9771.	0.7	565.
R-717-048HN	95.63	198.7	197.7	0.0681	93.95	20.07	4.6	2.5	16083.	83.07	87.32	4.22	10.43	9680.	9785.	1.1	527.
R-717-049HN	84.41	165.7	164.8	0.0176	81.90	5.28	34.0	18.3	115066.	83.30	83.48	0.15	1.02	2610.	2493.	-4.5	1455.
R-717-050HN	84.94	167.2	166.2	0.0180	82.96	5.40	17.7	9.5	59997.	83.35	83.68	0.30	1.42	2667.	2631.	-1.3	1064.
R-717-051HN	85.25	168.2	167.1	0.0183	83.30	5.46	13.3	7.2	45124.	83.37	83.82	0.42	1.66	2695.	2800.	3.9	922.
R-717-052HN	85.77	169.2	168.5	0.0177	83.56	5.31	8.3	4.5	28209.	83.39	84.08	0.66	2.03	2614.	2724.	4.2	731.
R-717-053HN	86.35	171.2	170.2	0.0182	84.02	5.43	5.1	2.8	17310.	83.07	84.18	1.08	2.73	2672.	2753.	3.0	556.
R-717-054HN	86.50	171.7	170.6	0.0181	84.13	5.41	4.5	2.4	15154.	82.91	84.15	1.22	2.97	2664.	2712.	1.8	509.

APPENDIX D

SI CONVERSION FACTORS

An attempt has been made to present all key tables and figures in dual units (ACU and SI). The following conversion factors may be used to convert from ACU to SI units:

To convert from	To	Multiply by
Btu/hr	W	0.2929
Btu/hr·ft^2	W/m^2	3.152
Btu/hr·ft^2·°F	W/m·K	1.730
Btu/hr·ft^2·°F	W/m^2·K	5.675
Btu/lb$_m$	J/kg	2.324×10^3
Btu/lb$_m$·°F	J/kg·K	4.184×10^3
ft	m	0.3048
ft^2	m^2	0.0929
ft/hr^2	m/s^2	2.35×10^{-8}
ft/sec	m/s	0.3048
gpm	m^3/s	6.309×10^{-5}
in.	cm	2,54
lb$_f$/ft	N/m	14.59
lb$_m$/hr·ft	Pa·s	4.134×10^{-4}
lb$_m$/hr·ft^2	Pa·s/m	1.356×10^{-3}
psia	Pa	6.895×10^3
Δ(°F)	Δ(K) or Δ(°C)	0.5556

Temperature conversion: $T(K) = 5/9 \times [T(°F) - 32] + 273.15$

$T(°C) = 5/9 \times [T(°F) - 32]$

ORNL-5488
Dist. Category UC-93

INTERNAL DISTRIBUTION

1. S. E. Beall
2. R. H. Chapman
3. F. C. Chen
4-11. S. K. Combs
12. W. B. Cottrell
13. F. A. Creswick
14. N. Domingo
15. D. M. Eissenberg
16. Harold Falkenberry, Consultant
17. W. Fulkerson
18. R. F. Hibbs
19-23. H. W. Hoffman
24. R. N. Lyon
25. R. E. MacPherson
26. G. S. Mailen
27. R. E. Males, Consultant
28-37. J. W. Michel
38. S. L. Milora
39. R. W. Murphy
40. F. R. Mynatt
41. H. Postma
42. R. C. Robertson
43. David J. Rose, Consultant
44. M. W. Rosenthal
45. M. R. Sheldon
46. V. Kerry Smith, Consultant
47. I. Spiewak
48. D. G. Thomas
49. H. E. Trammell
50. D. B. Trauger
51. Macauley Whiting, Consultant
52. D. G. Whitman
53. ORNL Patent Office
54-56. Central Research Library
57. Document Reference Section
58-59. Laboratory Records
60. Laboratory Records (RC)

EXTERNAL DISTRIBUTION

61. Assistant Manager, Energy Research and Development, DOE-ORO
62-235. Given distribution as shown in TID-4500-R66 under Energy Conversion
236. J. Hilbert Anderson, Sea Solar Power, Inc., 2422 South Queen Street, York, PA 17402
237. David Aronson, David Aronson Associates, 9 Riverview West, Upper Montclair, NH 07043
238. Professor Kenneth J. Bell, School of Chemical Engineer, Oklahoma State University, Stillwater, OK 74074
239. Professor A. E. Bergles, Department of Mechanical Engineering, Iowa State University, Ames, IA 50010
240. Dr. R. A. Bonewitz, Aluminum Company of America, Alcoa Labs. 7th Street Road, Route 780, Alcoa Center, PA 15069
241. Robert Douglass, Jr., TRW Systems and Energy Inc., One Space Park, Redondo Beach, CA 90278
242. Dr. Gordon L. Dugger, Applied Physics Laboratory, John Hopkins University, John Hopkins Road, Silver Spring, MD 20810
243. Sigmond Gronich, Division of Solar Energy, Department of Energy, 600 E Street, NW, Washington, DC 20545
244. Dr. R. Philip Hammond, R&D Associates, 4640 Admiratly Way, P.O. Box 9695, Marina del Rey, CA 90291
245. Donald Hornburg, DSS Engineers, Inc., 7483 Northwest 4th Street, Fort Lauderdale, FL 33317

246. Dr. Matthew Kelleher, Naval Postgraduate School, Department of Mechanical Engineering, Monterey, CA 93940
247. Eugene H. Kinelski, Ocean Systems Branch, Division of Central Solar Energy, Department of Energy, Washington, DC 20545
248. Professor James G. Knudsen, Engineering Experimental Station, Oregon State University, Covell Hall 219, Corvallis, OR 97331
249. Dr. Abrahim Lavi, Department of Engineering, Carnegie-Mellon University, Schenley Park, Pittsburgh, PA 15213
250. Ray I. Lindberg, Reynolds Metals, 4th & Canal Streets, Richmond, VA 32361
251. Dr. A. L. London, 4020 Amaranta Avenue, Palo Alto, CA 94306
252. Dr. Paul Marto, Naval Postgraduate School, Department of Mechanical Engineering, Monterey, CA 93940
253. Professor Jon G. McGowan, Mechanical Engineering Department, University of Massachusetts, Amherst, MA 01002
254. Bernard Messinger, 4162 Sunridge Road, Pebble Beach, CA 93953
255. W. C. Moore, York Division, Borg Warner Corp., York, PA 17403
256. Frank Notaro, Union Carbide Corp., Linde Division, P.O. Box 44, Tonawanda, NY 14150
257. Dr. W. L. Owen, Lockheed Missiles & Space Company, Inc., P.O. Box 504, Sunnyvale, CA 95088
258. Robert W. Perkins, Spiral Tubing Corp., 533 John Downey Drive, New Britain, CT 06051
259. Dr. H. F. Poppendiek, Geoscience, Ltd., 410 South Cedros Avenue, Solona Beach, CA 92075
260. Kenneth F. Read, Ocean Systems Branch, Division of Central Solar Technology, Department of Energy, 600 E Street, NW., Washington, DC 20545
261. William Richards, Ocean Systems Branch, Division of Central Solar Technology, Department of Energy, 600 E Street, NW., Washington, DC 20545
262. Dr. R. R. Rothfus, Chemical Engineering Department, Carnegie-Mellon University, Schenley Park, Pittsburgh, PA 15213
263. Norman F. Sather, Argonne National Laboratory, 9700 South Cass Avenue, Argonne, IL 60439
264. Professor Kenneth E. Starling, School of Chemical Engineering and Materials Science, Room 23, University of Oklahoma, 202 West Boyd, Norman, OK 73069
265. Dr. Armando Steinbruchel, Aqua-Chem, Inc., P. O. Box 421, Milwaukee, WI 53201
266. Lloyd C. Trimble, Lockheed Missiles & Space Company, Inc., P.O. Box 504, Sunnyvale, CA 94088
267. C. M. Zener, Department of Electrical Engineering, Carnegie-Mellon University, Schenley Park, Pittsburgh, PA 15213

☆U.S. GOVERNMENT PRINTING OFFICE: 1979-748-189/391